Digital Comprehensive Summaries of Uppsala Dissertations
from the Faculty of Science and Technology 2297

Illuminating Benzothiadiazole

Mechanistic Insights into its Role in Fuel-Forming Reactions

MARTIN AXELSSON

ACTA UNIVERSITATIS
UPSALIENSIS
2023

ISSN 1651-6214
ISBN 978-91-513-1877-6
urn:nbn:se:uu:diva-509537

UPPSALA
UNIVERSITET

Dissertation presented at Uppsala University to be publicly examined in Polhemsalen, Ångströmslaboratoriet, Lägerhyddsvägen 1, Uppsala, Friday, 6 October 2023 at 09:15 for the degree of Doctor of Philosophy. The examination will be conducted in English. Faculty examiner: Professor Ksenjia Glusac (University of Illinois, Chicago).

Abstract
Axelsson, M. 2023. Illuminating Benzothiadiazole. Mechanistic Insights into its Role in Fuel-Forming Reactions. *Digital Comprehensive Summaries of Uppsala Dissertations from the Faculty of Science and Technology* 2297. 90 pp. Uppsala: Acta Universitatis Upsaliensis. ISBN 978-91-513-1877-6.

Development and understanding of catalytic reactions involved in fuel formation are crucial to be able to make the energy transition into a sustainable future. One intriguing type of catalyst for these types of reactions is organic material catalysts, which combine some of the tunable nature of molecular catalysts with the scalability and robust nature of material catalysts. The understanding of the catalytic mechanisms in these types of materials is still a work in progress. In the last decade D-A type polymers have gotten a lot of attention as potential photocatalysts for fuel-forming reactions but currently, the mechanisms in which these reactions take place are very limited.

This thesis focuses on the molecular unit benzothiadiazole (BT) and its role in catalytic fuel-forming reactions across various molecules and polymers. In paper I: The hydrogen evolution reaction (HER) is investigated on the small molecule 2,1,3-benzothiadiazole-4,7dicarbonitrile (BT). The study reveals that BTDN serves as an electrocatalyst for the HER. Some catalytic intermediates were identified spectroscopically and a catalytic mechanism was proposed.

In papers II and III: Polymeric nanoparticles (Pdots) based on the polymer poly(9,9-dioctylfluorene-alt-2,1,3-benzothiadiazole (PFBT) were investigated for photocatalytic fuel-forming reactions. First, the HER was explored and it emphasised the significance of proton binding to the BT unit as a catalytic intermediate. It also showed that changing to basic conditions can quench the HER and make place for CO2 reduction to CO and that PFBT Pdots exhibit good selectivity in catalyzing this reaction.

Finally, in Paper IV, the binding and reduction of CO2 on the molecule BTDN were investigated. It was shown that BTDN can bind CO2 in multiple reduced states and reduce it to CO and oxalate in a third reduction, albeit with seemingly low efficiencies.

Keywords: Photocatalysis, Electrocatalysis, Renewable Energy, Mechanistic Studies, Cyclic Voltammetry, Benzothiadiazole

Martin Axelsson, Department of Chemistry - Ångström, Physical Chemistry, Box 523, Uppsala University, SE-75120 Uppsala, Sweden.

ISSN 1651-6214
ISBN 978-91-513-1877-6
URN urn:nbn:se:uu:diva-509537 (http://urn.kb.se/resolve?urn=urn:nbn:se:uu:diva-509537)

The cosmos is within us. We are made of star stuff. We are a way for the universe to know itself - Carl Sagan

List of papers

This thesis is based on the following papers, which are referred to in the text by their Roman numerals.

I **Small Organic Molecule Based on Benzothiadiazole for Electrocatalytic Hydrogen Production**
Martin Axelsson, Cleber F. N. Marchiori, Ping Huang, C. Moyses Araujo, and Haining Tian. **2021**
Journal of the American Society, 2021, 143, 21229-21233.
Contribution: I contributed to the planning of the study, I performed all experiments except the EPR measurements which I assisted on. I did all of the data analysis and the simulated data and helped with the interpretation of the DFT calculations. I wrote the initial draft of the manuscript and contributed to the interpretation of the results.

II **The Role of Benzothiadiazole Unit in Organic Polymers on Photocatalytic Hydrogen Production**
Martin Axelsson, Ziyang Xia, Sicong Wang, Ming Cheng, and Haining Tian. **2023**
ChemRxiv Preprint Manuscript
Contribution: I contributed to the planning of the study, I performed all electrochemical experiments and the pH-dependence study of the photocatalytic experiments including Pdot preparation. I did the data analysis of all my own data and the data simulations. I wrote the initial draft of the manuscript and contributed to the interpretation of the results.

III **Organic Polymer Dots as the Photocatalyst for CO2 Reduction in Aqueous Solution**
Bin Cai, Martin Axelsson, Mariia V. Pavliuk, Sicong Wang, Haining Tian **2023**
Resubmitted Manuscript
Contribution: I performed the SEC and voltammetry experiments and did the data analysis. I contributed to the discussion and planned complementary experiments. I contributed to the result interpretation and the final version of the draft.

IV **A Benzothiadiazole Based Molecule for CO_2 Capture and Reduction in Multiple Reduced States**

Martin Axelsson, Carlos Enrique Torres Mendez, Mun Hon Cheah, and Haining Tian. **2023**
Manuscript
Contribution: I contributed to the planning of the study, I performed all of the cyclic voltammetry and SEC measurements. I did the majority of the data analysis. I wrote the initial draft of the manuscript and contributed to the interpretation of the results.

Reprints were made with permission from the publishers.

Papers not included in the Thesis

Panchromatic ternary polymer dots involving sub-picosecond energy and charge transfer for efficient and stable photocatalytic hydrogen evolution
Aijie Liu, Lars Gedda, Martin Axelsson, Mariia Pavliuk, Katarina Edwards, Leif Hammarström, Haining Tian **2021**
Journal of the American Society, 2021, 143, 2875-2885.

Preparation, characterization, evaluation and mechanistic study of organic polymer nano-photocatalysts for solar fuel production
Mariia V Pavliuk, Sina Wrede, Aijie Liu, Andjela Brnovic, Sicong Wang, Martin Axelsson, Haining Tian **2022**
Chemical Society Reviews, 2022, 51, 6909-6935.

Contents

Acronyms

AcA	Acetic Acid
AcN	Acetonitrile
AscA	Ascorbic Acid
BT	Benzothiadiazole
BTDF	2,1,3-benzothiadiazole-4,7-di-9,9-dioctylfluorene
BTDN	2,1,3-benzothiadiazole-4,7-dicarbonitrile
CO_2RR	Carbon dioxide reduction reaction
CE	Counter electrode
COF	Covalent organic framework
CV	Cyclic voltammetry
DEA	Diethylamine
DLS	Dynamic light scattering
EPR	Electron paramagnetic resonance spectroscopy
FTIR	Fourier transform infrared spectroscopy
GC	Glassy carbon
HER	Hydrogen evolution reaction
MOF	Metal-organic framework
NMR	Nuclear magnetic resonance spectroscopy
OLED	Organic light-emitting diode
OPV	Organic photo-voltaic
PCBM	Phenyl-C61-butyric acid methyl ester
PFBT	poly(9,9-dioctylfluorene-alt-2,1,3-benzothiadiazole)
PSII	Photosystem II
RE	Reference electrode
SAL	Salicylic acid
SEC	Spectro-electro chemistry
SD	Sacrificial donor
TEA	Triethylamine
TEOA	Triethanolamine
THF	Tetrahydrofuran
WE	Working electrode

1. Introduction

1.1 The Energy Crisis

The world stands on the brink of a cataclysmic event in the form of a complete environmental collapse. Humanity has exponentially increased its mark on nature and pushed the earth toward its planetary boundaries, the lines that when crossed, there is no turning back [1, 2]. We are changing the earth in terms of its geology and ecology so much that climate researchers call it a new epoch, the Anthropocene [3]. To avoid irreversible changes and keep our home a place where life in its current form flourishes, it is clear that we need to stop exploiting nature and move to a sustainable society. The biggest culprit for the rapidly changing climate is our over-reliance on fossil energy sources. These hydrocarbons have amassed from decaying biomass in the pressure of the earth's crust over millennia. They are also storage of carbon dioxide from the earth's baby years when the earth had a much less gentle climate. It turns out that burning these ancient molecules is a fantastic source of easily accessible energy, however, it also comes with many unacceptable downsides.

The products from the combustion of hydrocarbons are water and carbon dioxide, incomplete combustion will also make side products like NO_x, methane and carbon particles. Most of these molecules have large absorption bands in the infrared region of the electromagnetic spectrum, the region of the spectrum where heat is transferred. The fact is that an increase of CO_2 in the atmosphere would increase the temperature of the planet due to the retention of the heat that would otherwise be reflected out into space. This phenomenon is called the greenhouse effect and the contribution that increased CO_2 concentration has on the warming effect was first recognized by Svante Arrhenius already back in 1896 [4]. So it is clear that while the importance and danger of a temperature increase took longer to realize, we have understood the outcome of releasing CO_2 into the atmosphere for over a century. The argument for regression to a pre-industrial society can be made to stop these emissions. This is, however, not a path that many people would find acceptable. The path forward then, has to be a radical transition from fossil to renewable energy sources to achieve a complete stop of excess carbon emissions in the coming few decades. According to the best predictive scenarios we do not only need to stop the use of fossil fuels but also start removing carbon dioxide and other greenhouse gases and go below net zero in greenhouse gas emission in the coming three decades [5].

The by far most abundant energy source, renewable or not, is the sun [6]. Every year, more energy reaches the earth in the form of sunlight than the entire known reservoir of fossil resources, and counting the energy of wind, hydro and biomass, which are all generated by the sun. The switch then is more a question of investment into renewable energy sources than a question of where the energy can come from. However, solar energy comes with a big flaw, it only works when the sun is shining. The solution to the intermittent nature of solar energy (which also applies to wind power) is storing the energy when it is available to compensate for the downtime. Storing energy is not a trivial pursuit, especially electricity. And currently the most effective technology that is available to capture solar energy generates electricity through the use of photovoltaics [7]. While batteries will be part of the solution, especially with the development of high-capacity lithium-ion batteries, the energy density of batteries is still much lower than the fuels that are currently in use [8]. An alternative way to store energy that we already have well-functioning technologies and infrastructure to make use of is to store it in highly energetic chemical bonds. In other words, to make renewable fuels.

Since the most abundant renewable energy source is the sun and perhaps the most promising way of storing energy is in chemical bonds it makes sense to combine the two. This class of fuels based on solar energy is aptly called solar fuels. Generating these types of fuels is a process that is at the moment an emerging technology with a wide scope of possible paths to get to the goal. To be able to find the best possible solutions, we both need to invent systems for the transformation and develop an understanding of the processes to build on successful systems. In this thesis, I describe the work I have done in understanding the fundamental fuel-forming processes of organic molecules based on the molecule 2,1,3-benzothiadiazole, as seen in Figure 1.1.

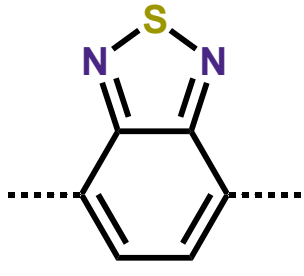

Figure 1.1. The chemical structure of 2,1,3-benzothiadiazole with bonds at the 4, 7 positions on the benzene ring with alternative groups in the different molecules studied in this thesis.

1.2 Photosynthesis

The process of converting solar energy and saving it in chemical bonds is not a novel idea, in fact, this exact process is the foundation of all life on earth. Photosynthesis is the process of how nature utilizes the energy of the sun to convert carbon dioxide and water to glucose, and later into larger carbohydrates, and oxygen. While the overall reaction might seem simple, the reality is a complex chain of light receptors, electron transfer mediators, catalytic centres, proton gradients, and energetic carrier molecules such as ATP and NADPH. an overview of how the system is currently understood can be seen in Figure(1.2) [9, 10].

The natural system's complexity leads to a low energy conversion efficiency often less than 1% [11], something that would need to be improved to use this as an applicable energy conversion method. Even more importantly, the complexity of the natural system hints at the difficulty of making the reaction proceed in the correct direction. This comes from the fact that at every step the high energy charge-separated state has a driving force to recombine and release the energy back as light or heat. To generate high-energy fuels we must overcome the same issues as in nature. We must learn how to direct multiple charges from stable compounds into high-energy compounds without them returning to the same spot, but we must beat nature in energy efficiency, which is no small task.

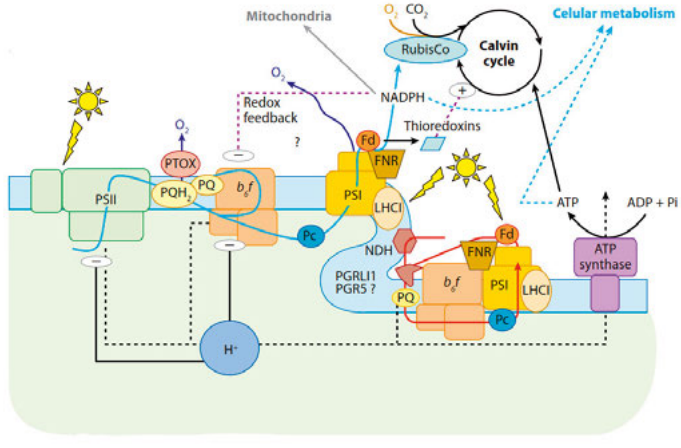

Figure 1.2. A cartoon of the overall photocatalytic reaction, the blue arrow indicates the photocurrent, the overall pathway of the photogenerated electrons. The reaction starts in photosystem II (PS II) and ends with the Calvin cycle where the CO_2 is reduced and converted into glucose. Recreated with permission from Annual Review of Genetics.

1.2.1 Artificial Photosynthesis

To beat nature in its processes we must first understand how to replicate the chemistry it is performing. The field of science that has taken up this task is called artificial photosynthesis. Artificial photosynthesis is a broad umbrella of concepts based on the same general idea of converting solar energy into high-energy chemicals. In contrast to the natural system, the products are typically way simpler molecules than hydrocarbons. One of the main reactions pursued is water splitting [12], the separation of water into molecular hydrogen and oxygen (1.1). H_2 is a high-energy product that can be both used as a fuel in itself but can also be used as a valuable feedstock for industrial synthesis. This reaction has the desired feature of being completely cyclic as the product of H_2 combustion or oxidation in a fuel cell is again H_2O.

$$\begin{aligned} &2\,H_2O \rightleftharpoons 2\,H_2 + O_2 \\ &\text{---------------------------} \\ &2\,H_2O \rightleftharpoons 4\,H^+ + 4\,e^- + O_2 \\ &4\,H^+ + 4\,e^- \rightleftharpoons 2\,H_2 \end{aligned} \tag{1.1}$$

The reaction is typically divided into two sub reactions the oxidation of H_2O to O_2 and the reduction of protons to H_2. The separation of the oxidation and reduction reaction makes sense from what they demand from both an energetic and kinetic perspective and is typically performed at separate sites in the photosynthetic system. Another reaction that is of large interest in the field is that of reducing CO_2 and transforming it into high-energy carbon fuels or chemicals. The targets are molecules such as methanol, ethanol, ethylene, and later on more complex molecules such as jet fuels, plastics and medicines [13]. In theory, this reductive step could just replace the proton reduction step in water splitting while still taking the electrons from the oxidation of water. However, the entire chemical system would have to be re-suited to fit the new reactions in mind.

The overall scheme is quite general, the oxidation could also be swapped out to do something valuable instead of just producing oxygen. An overall general scheme of the artificial photosynthetic reaction can be seen in Figure 1.3. Approaches to make these reactions happen range from systems with very little in common with natural photosynthesis, such as photovoltaics coupled to electrolyzers, to more direct mimics of the natural system with molecular setups resembling those found in the photosynthetic process. There are even approaches to hijack the biological photosynthetic machinery to utilize it for the production of valuable chemicals. Each approach comes with its own set of advantages and challenges.

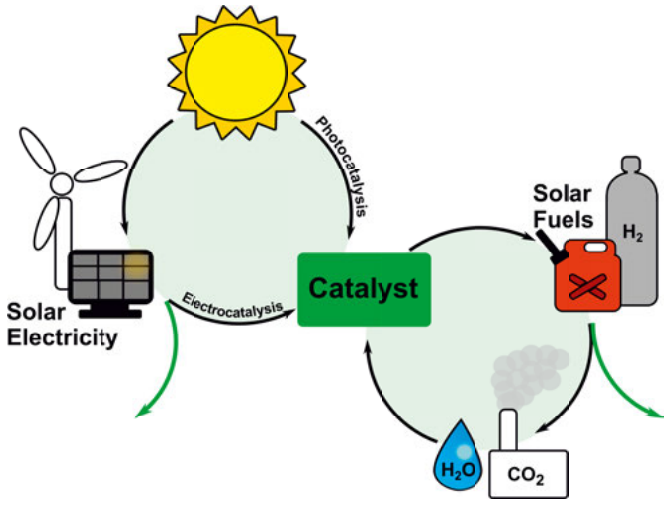

Figure 1.3. A cartoon of the general scheme for artificial photosynthesis, taking either the direct photocatalytic approach or the indirect electrocatalytic approach through the generation of solar electricity. The cyclic nature of the reactants and products for the generation of solar fuels is key to the sustainability of the process so that in the end the only input is the energy of the sun (and if that stops we have bigger issues than a renewable energy supply).

1.3 Catalysis in Fuel-Forming Reactions

Common to each approach of artificial photosynthesis is that they require a catalyst that can assist the chemical transformations, reducing their energetic barriers and increasing the rate at which they progress [14]. The general function of a catalyst is easiest described with transition state theory, where Arrhenius equation 1.2, shows that the rate of a chemical reaction, k is determined by the activation energy of the transition, E_a [15, 16].

$$k = Ae^{-E_a/RT} \tag{1.2}$$

A catalyst speeds up the reaction by lowering the energy barrier to the transition state without itself being altered in the reaction. A scheme of catalytic systems can be seen in Figure 1.4, where the energy barrier is aptly described as units of free energy. The complication that makes fuel-forming reactions extra difficult is that the product will be more energetic than the starting products, this means that the catalyst needs to be activated by an energy influx to be able to make the reaction energetically feasible.

Overall, the full scale of the reaction follows the general reaction scheme with a total negative ΔG^0 with the exception being that the chemical system with the reactants needs to be activated to a higher energy level before the reaction can occur. This energy will come from high-energy electrons or holes,

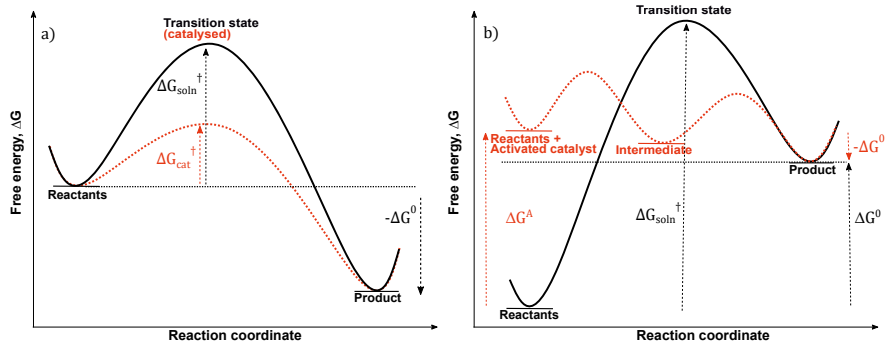

Figure 1.4. Energy diagrams of catalysed and uncatalysed reactions both in a general (a) case and in the case of a fuel forming reaction (b) where the catalyst is first activated by an external energy source ΔG^A. The catalyst reduces the energy barrier $\Delta G^{\dagger}_{soln}$, required for the chemical transformation and instead takes the pathway of the catalysed transition state which requires less energy in $\Delta G^{\dagger}_{cat}$, the lower energy pathway speeds up the overall reaction. The wavy potential surface in b) is closer to a real case of catalysis where the reaction transpires through one or several intermediates.

generated by light, in the case of photosynthesis, or due to high potential electrons generated from an external power source in the case of electrocatalysis. Due to the high energy of the activated complex, there is a high likelihood that the high-energy electron will move back to its initial low-energy state [17]. To prevent this recombination the intermediates formed in conjunction with the catalyst need to be sufficiently stable. However, if the intermediates would be too stable it would impede or stop the catalytic process. Fitting this parameter is a key step in determining the catalytic activity of the catalyst. The catalysts that fit all of these demands typically form into two categories, materials, and molecular catalysts including enzymes. The stabilization of the catalytic intermediates is well described with a binding energy volcano plot in material catalysis [18]. The concept that the catalytic rate is dictated by how strongly bound the substrates are in the intermediates is also true for molecular catalysts.

1.3.1 Molecular Catalysts, Tunability and Selectivity

Molecular catalysts have the advantage of an extremely tunable catalytic site with the opportunity to modify not only the binding coordination of the catalytic substrate but also the second and third coordination sphere [19–22]. This has been shown to be of key importance and is especially clear when looking at natural enzymes. In natural fuel-forming reactions, the enzyme typically has a molecular cofactor active site that is surrounded by a strict protein fold. Examples of such proteins are the PSII with its, Mn_4CaO_5 active site [23],

and [FeFe]-hydrogenases with their cofactor [20, 24, 25]. Both cofactors lose much of their activity or become completely unstable when removed from their protein scaffold [24, 26]. This feature of a well-controlled active site can be so specific that it enables this type of catalyst to be selective towards single reaction products. Selectivity is especially important when reducing CO_2 for two reasons, protons are required for most desired products from the reduction process so hydrogen evolution will be a competing process [27, 28].

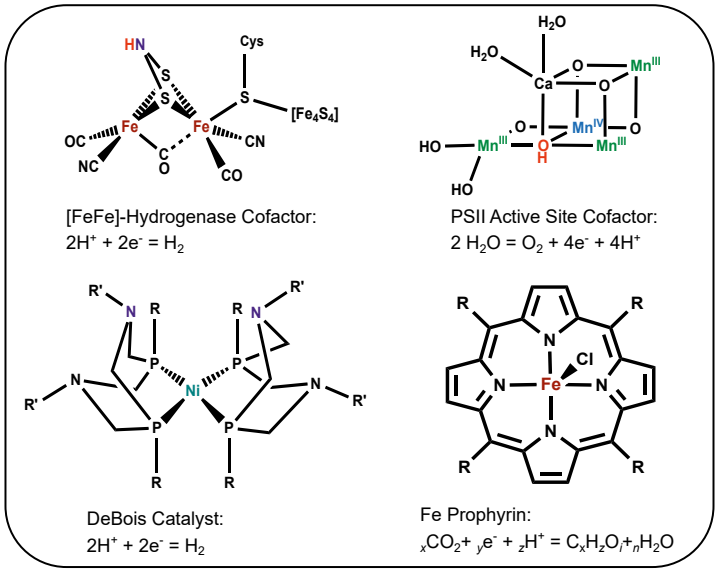

Figure 1.5. Four molecular catalyst and enzymatic catalytic sites and the main catalytic reaction they perform.

The second problem is that the thermodynamic potential for many of the CO_2 reduction pathways are very similar, see Figure 1.6, so a mixture of products is likely from a catalyst with low selectivity. The best synthetic catalysts often take inspiration from the enzymatic active sites, with examples such as the DuBois catalyst that is highly inspired by the [NiFe]-hydrogenase active site with nitrogen-centred proton shuttles to the metal centre, and the large group of metalloporphyrins mimicking the binding site of O_2 and CO in haemoglobin, their structures are shown in Figure 1.5 [19, 29–33].

In materials the tunability is much more limited; the well-defined binding energies on material surfaces for reactants and catalytic intermediates typically increase linearly leading to linear scaling relationships away from where the most active catalytic process would occur [34]. Typically the active site for catalysis in materials is also much more elusive and difficult to study but most often occurs at kinks and edges on the material surface. However, materials

Nr:	Reaction:	E° vs SHE:
1	$CO_{2\,(aq)} + e^- \rightarrow CO_2^{\bullet-}{}_{(aq)}$	-1.90 V
2	$CO_{2(g)} + 2H^+ + 2e^- \rightarrow HCOOH_{(aq)}$	-0.61 V
3	$CO_{2(g)} + 2H^+ + 2e^- \rightarrow CO_{(g)} + 2OH^-{}_{(aq)}$	-0.52 V
4	$CO_{2(g)} + 4H^+ + 4e^- \rightarrow HCHO_{(g)} + H_2O$	-0.48 V
5	$CO_{2(g)} + 6H^+ + 6e^- \rightarrow H_3COH_{(g)} + H_2O$	-0.38 V
6	$CO_{2(g)} + 8H^+ + 8e^- \rightarrow CH_{4(g)} + H_2O$	-0.24 V
7	$2H^+ + 2e^- \rightarrow H_{2(g)}$	0 V

Figure 1.6. The thermodynamic redox potentials for the CO_2RR compared to SHE at pH 7 and 25^{o}C with 1 atm gas pressure and 1 M of solvated species [27, 28]. Displaying that most products are within a potential window of 0.4V, well within the over-potential required to run these reactions at high activities.

come with many benefits over the molecular systems outside of the selectivity and activity.

1.3.2 Material Catalysts, Robustness and Scalability

A catalyst that would be practically applicable does not only have to be very active it also has to fit the overall chemical system where it should be applied, often some sort of device like an electrolyser or photoelectrode. Critically the catalyst also needs to be robust so that the device performing the chemical reaction can be in use for a long time. The stability and ease of integration in a device are where material catalysts outperform their molecular counterparts by far, while there are successful attempts there are many problems with integrating molecular catalysts onto electrode surfaces [35]. There are now multiple scaleable methods for material synthesis that can be applied directly to electrodes, and while direct structural tuning in material synthesis is still difficult, control over nano-structures is more and more accessible[36–38].

While the selectivity becomes a big issue for more complex reactions like the water oxidation reaction and the CO_2 reduction reactions (CO_2RR) there are some reactions that are essentially optimised on material surfaces such as the hydrogen evolution reaction (HER) on platinum that is right at the top of the volcano plot [39]. Copper is also exceptional with its affinity to catalyse the formation of C-C bonds from CO_2 which allows C2+ products [40], however, it is also infamous for giving a huge mixture of carbon products from the catalysis which in part is due to the unspecified active site and the difficulty of tuning the surface for specific products [34, 36]. It is also well documented that metallic catalysts are not static during the catalytic process [41, 42], so even if the surface would be specifically tailored for a reaction it does not

mean that it would stay that way in operado conditions.

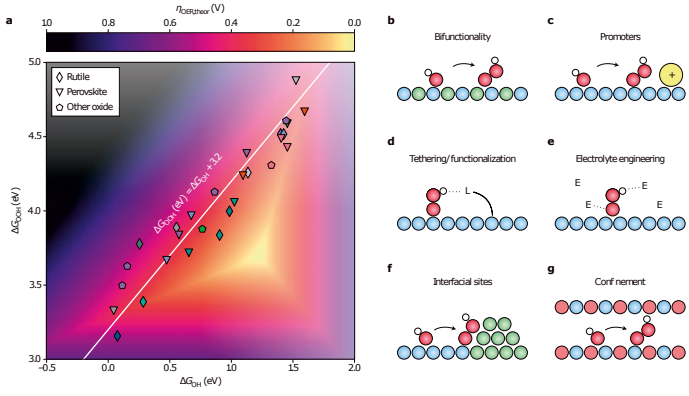

Figure 1.7. The scaling relationship of metal oxides as catalysts for the water oxidation reaction, as well as multiple suggested ways of breaking the scaling relationship by modifying the electrode surface. Recreated from Montoya *et al.* [34] with permission from Springer Nature.

There are several approaches applied to try and combine the benefits of molecular and material catalysts and make systems that are active, selective, robust and scaleable. Three widespread approaches are the incorporation of molecular catalysts on conducting electrodes, and in metal-organic frameworks (MOFs) [43–46]. The incorporation of catalysts in conductive electrodes is perhaps the simplest idea, often utilizing highly porous semiconductors or carbon-based materials such as nanotubes as a scaffold. The approach has such a huge span of combinations but it is often difficult to predict how the catalyst will act when anchored to the structure. On an electrode surface, the molecule will have stearic limitations as compared to a solution or protein scaffold, and the strong electric field at the electrode surface has been shown to alter the electronic structure to a large degree [47, 48]. MOFs offer an enormous surface area and a well-defined structure where molecular catalyst moieties are easily incorporated, however, the tight porous structure limits the mass transport of substrates and products in the framework [49]. MOFs also have the complication, similarly to molecules on electrodes, of largely affecting the electronic structure and chemical surrounding of the molecule which can change its properties radically.

Another approach to combine the tunable nature of molecular catalyst with material properties are organic material catalysts. For as long as chemistry has been a real field of science the masters of synthetic chemistry have been the organic chemist. Due to the flexible nature of carbon, the varieties of structures that can be synthesised are gigantic, and several organic materials have

displayed impressive catalytic capabilities including graphitic carbon nitrides, covalent organic frameworks (COFs) and semi-conducting polymers [50–55].

1.4 Organic Material Catalysts

Fully organic catalysts are not a new thing, most of all enzymes in nature are completely metal-free, however, most redox-active enzymes contain a metal-centred cofactor. The first metal-free photocatalytic material was discovered already back in the 80s with the polymer Poly(p-phenylene) shown to work as being active for the HER but the research did not spark a huge interest in the scientific community due to a large band gap and moderate activity [56, 57]. It was not until 2009 when Wang et. al. [58], reported photocatalytic activity from graphitic carbon nitride that the field got a kick start. Since then there has been huge progress in developing graphitic carbon nitrides, trying to overcome the main flaws such as a large band gap and limited tuneability. But the field has also branched out and started a huge interest in other organic photocatalysts. This renewed effort has led to discoveries of a large variety of semiconducting polymers and COFs have been reported [52–55], as catalytically active materials, mostly for photo-catalytic HER. COFs and conjugated polymers share many features except their dimensionality as COFs are three-dimensional whereas polymers are one or two-dimensional in their structure. In the following section, I will focus on polymers but many of the features are true for catalytic COFs as well.

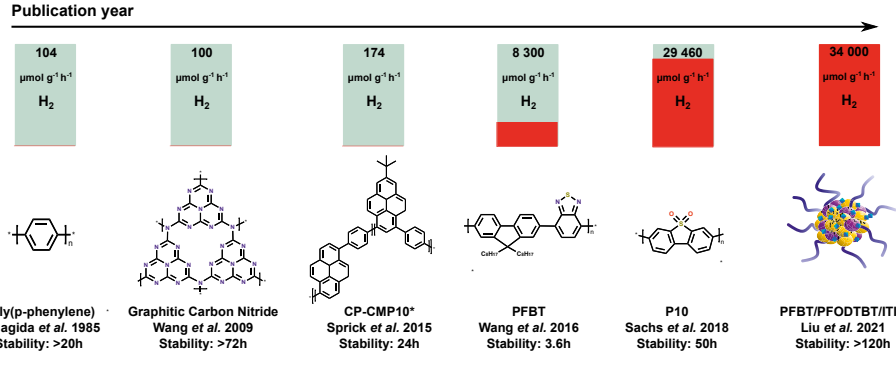

Figure 1.8. A short timeline of the development of organic material photocatalysts for the HER, with PPP in 1985 [56], the first paper of graphitic carbon nitride [58], the reintroduction of polymeric systems (*2D representation of the material) [59], the first application of Pdots for better suspension [60], the development of highly efficient single polymers [61], and the utilization of multiple heterojunctions in a particle [62].

1.4.1 Conjugated Donor-Acceptor Polymers

The connecting feature in all of these materials is their high degree of conjugation, which allows for high electron mobility compared to other organic materials. All of these polymers, importantly, share the feature of a donor-acceptor or push-pull structure. This is a type of structure where electron-rich and electron-poor moieties are alternated, which leads to a strong electronic connection in the material's backbone [63–65]. It also means that the materials easily form excitons upon excitation by light which can easily be reduced or oxidised. This type of structure is also common in dyes and is notable for its often very high extinction coefficients, in fact, many of the same polymers that have been used as photocatalysts are also used in organic photovoltaics (OPVs) as well as organic light-emitting diodes (OLEDs) for the same reasons [65–67].

While studying a photocatalyst it is typically only for one half-reaction at the time due to the different demands of the catalytic reactions. This leads to the use of sacrificial agents, molecules that are easily reduced or oxidised depending on the counter-reaction, so for HER sacrificial donors (SDs) are used [68]. The role of the sacrificial agent is to not interfere with the catalytic process but is only present to mimic the electronic property of the other half-reaction. The inclusion will change the chemical environment substantially, and it will also dictate features of the chemical system such as pH and ionic strength conditions that may or may not be applicable to the finalized catalytic system.

A drawback for these polymeric systems is that they are typically very hydrophobic which is a large problem when the main reaction they are being studied for is the HER from water. Early systems overcame this issue by utilising a solvent mixture of water and methanol, and high concentrations of sacrificial donors [59, 69, 70]. While many of these systems showed promise the optical density of the suspension was often a problem due to high degrees of light scattering. A way to overcome this challenge was introduced by Wang et al. in 2016 where they utilised the concept of surfactant-assisted polymer nano-particles called polymer dots or Pdots [55, 60], previously used as fluorescent probes in cells. The inclusion of amphiphilic polymer surfactants makes the particles highly dispersible in pure water solutions without any problems with scattering. The high surface and increased hydrophilicity have allowed Pdots to reach overall higher activities compared to the previous suspensions as well.

Another problem with these photocatalytic systems is their short lifetime and poor light stability, something that has always been a problem with organic light absorbers [71, 72]. This is often attributed to the poor charge mobility in

the systems as compared to inorganic semiconductors which leads to charge accumulation inside of the polymer and in turn to degradation of the polymer. In theory, this could be alleviated by increasing the catalytic turnover to quickly use the charges before they start degrading the system. Though there has been steady progress in both performance and stability the field is still missing key information to be able to make significant improvements [73]. Specifically, a mechanistic understanding of how the chemical structure and environment affect the catalytic properties is required.

A point of investigation for these polymers is the role of palladium in HER. Pd will almost always be present in small amounts in the polymer, as a residual from the Suzuki-Miyaura coupling reaction that is used to synthesise them [74, 75]. It has been confirmed that the residual Pd plays a role in the HER for at least a few of the polymer-based systems [76, 77]. However, it has also been seen that for some polymers, that do contain a substantial amount of Pd, the photocatalytic activity is still very low or absent [78, 79]. This implies that what happens in the polymer structure, especially the acceptor unit is key to understanding the mechanisms of the reaction and why certain structures outperform others.

One thing that has been made clear in the last few years is that also the catalytic performance in these types of systems is severely limited by slow exciton diffusion through the polymers [80, 81], charge separation occurs locally in the polymer backbone and often has ultrafast recombination rates. A successful route to get around the problem has been to introduce heterojunctions with mixed polymer systems to have charge separation occur in between the different polymer structures and finally to add co-catalysts that utilize the charges for the HER [62, 82–84]. This strategy has also been shown to improve the overall catalytic stability and longevity of the systems. In these types of systems, the photophysics of the organic components is the most important factor since their only purpose is to absorb light and facilitate charge separation. However, there are still polymeric systems that function as decently efficient catalysts even without extra added catalysts, in these systems the chemistry that occurs on the polymer backbone becomes a key factor in the catalytic process.

The understanding of the chemistry that occurs on the polymeric backbone was the initial motivator of this thesis and the polymer of choice was poly(9,9-dioctylfluorene-alt-1,2,3-benzothiadiazole (F8BT or PFBT) that was the initial polymer to show high activity in the form of a Pdot. In this polymer, the electron acceptor moiety is benzothiadiazole (BT) a unit that has been highly successful in many of these types of D-A polymers. It was predicted that any chemical reaction occurring on the polymer backbone would be centred on the BT unit, as when the polymer was activated, either excited or reduced, most

of the electron density would be centred on the BT [78].

1.5 Benzothiadiazole as an Electron Acceptor

2,1,3-benzothiadiazole is one of the most widely used electron acceptors in D-A-type polymer structures and was first used in a polymer by Mullekom *et. al.* in 1996 [85]. It has since then been included in some of the most efficient OPVs, OLEDs, non-fullerene acceptors and organic photocatalysts known to date [54, 86, 87]. The reason for its success is the unique electron-withdrawing ability of the electron-deficient thiadiazole structure, as well as the tight conjugation with the benzene ring that makes it easy to incorporate into larger conjugated structures with strong electronic coupling [88]. The ability to modify it at the 4-7-sites of the benzene ring to different conjugations as well as at the 5-6-sites to modulate the electron-withdrawing properties has also helped its rise to prominence.

Before the work in this thesis, little was known about the redox chemistry that can be performed on the moiety, with the majority of studies focusing on its optoelectronic properties. The investigation of this acceptor unit in polymers would also lead to a neighbouring field of small organic molecules as catalysts for fuel-forming reactions.

1.6 Small Organic Catalysts

Even though the synthetic control of small molecule synthesis has led to an expansive library of catalysts, the vast majority of these have a metal ion in the centre. There are good reasons for this as the many possible redox states of the metal centre are able to accumulate the many charges that are required in all fuel-forming reactions. There are, however, ways around this where multiple charges can be stabilised in extended conjugated systems. And there are certain approaches that use small organic molecules for all of the most typical fuel-forming reactions such as water oxidation [89, 90], HER [91–94], and CO_2RR [95–97]. Common for all of these catalysts is that they are highly conjugated and nitrogen-rich systems, see Figure 1.9. The nitrogen sites function as important modulations of the electron structure due to their high electronegativity, which is important to modulate hydride strength either the HER or CO_2RR depending on the hydricity [95, 98]. The nitrogen sites can also act as protonation sites to generate catalytic intermediates that are crucial for the same reactions.

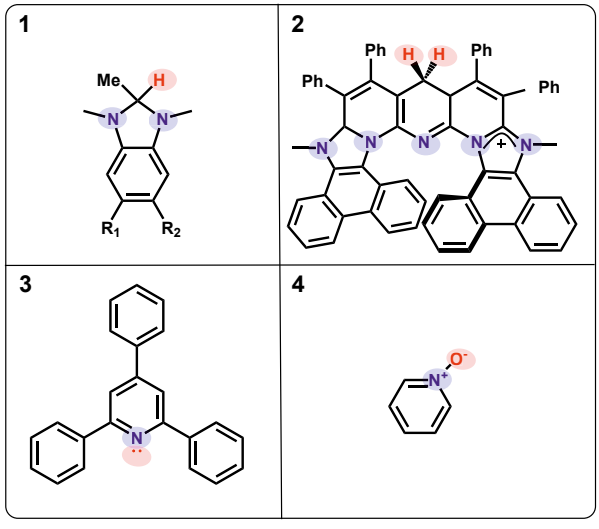

Figure 1.9. The chemical structures of some small organic catalysts with marked N atoms (blue) and active sites (red) in the structure. 1) A benzimidazole hydride, MeBIMH ([95, 96]) and 2) bis-imidazolium-embedded heterohelicene hydride ([94, 97]) capable of catalysing the CO_2RR and the HER, 3) 2,4,6-triphenylpyridine capable of catalysing the HER [92], and pyridine-N-oxide capable of catalysing water oxidation [90].

The field however is still in its infancy and very few parameters have been explored in these types of systems. All of the catalysts are also severely limited by some different properties. Water oxidation in general is often limited by high energetic barriers due to the complex kinetics of removing four electrons and four protons, often leading to high energy intermediates [36, 99]. The same problem exists for the small organic versions of this type of catalyst as well while they do not offer any significant advantage over their metal-centered or material-based versions. However, the pyridine-N-oxyl radical cation investigated by Li et. al. [90] shows promise as it has the ability to oxidise water to hydrogen peroxide instead of O_2 through a HAT mechanism, which could be a valuable mechanism to build on. For CO_2RR there has been a range of impressive hydrides developed in the last few years that selectively can generate formic acid completely avoiding the typical side products of H_2 and CO [96, 97]. However, these hydrides suffer from incredibly sluggish kinetics, especially in the regeneration of the hydride species, which has limited their ability to generate catalytic equivalents of the product. Currently, these results also indicate unfavourable comparisons to metal-organic complexes in terms of overpotential. Addressing this issue will be essential in forthcoming advancements. For hydrogen evolution the main problem seems to be stability [92–94], the most efficient catalysts reported only have faradaic efficiencies in the range of 80-90% and turnover numbers below 500 and these cat-

alysts also require a substantial overpotential to operate. One of them, 2,1,3-benzothiadiazole-4,7-dicarbonitrile (BTDN) is later described in this thesis.

While the current catalysts in this class are still leaving much to be desired, the landscape of these types of catalysts is still almost completely unexplored with just a handful of catalysts of each type described in literature. Even if none of these types of catalysts will find practical use, there is still much to learn about catalytic processes for reactions based on organic materials or ligand-based reactions in organo-metallic complexes. There is also an emerging field of utilising small organic molecules to modify the catalytic properties of material catalysts [100, 101].

2. Theory & Methodology

2.1 The Electronic Structure of Molecules

To understand what is happening in catalytic chemical reactions, it is key to understand the chemical processes at a level of bond formation. Essentially, all molecular bonds and chemical reactions are dictated by the energetic landscape and charge density distribution of the electronic orbitals. These orbitals are best described by the wave functions in Schrödingers equation (eq 2.1) [102], or equivalent matrix [103], or path integral formulations [104]. While methods to calculate the chemical structures are becoming more and more powerful, and are used to certain extents in the thesis, the only way we can experimentally look at these structures is indirectly through the quantum transitions that the electron will perform when excited by electromagnetic radiation.

$$i\hbar\frac{\partial}{\partial t}\Psi(\mathbf{r},t) = \hat{H}\Psi(\mathbf{r},t) \tag{2.1}$$

2.1.1 Electronic and Vibrational Spectroscopy

The quantum transitions inside molecules are studied by excitations driven by vibrations in the electromagnetic field or more simply, light, these are the fundamentals of spectroscopy. The type of transition that can be probed depends on the energy range of the light that is inducing the transition, typically referred to in terms of the frequency of the photon is directly proportional to its energy 2.2.

$$E = h\nu \tag{2.2}$$

Light can also be described by its wavelength, λ, which is proportional to the inverse of the frequency through 2.3. Even though the frequency has the benefit of being directly proportional to the energy most spectroscopic measurements are in the scale of wavelength.

$$\lambda = c/\nu \tag{2.3}$$

The information that can be gained from the spectroscopic measurement depends on how the experiment is arranged, the overall alignment of the light source or sources and the detector. The most common form of spectroscopy is

an absorption measurement where the absorbed light can be seen as a difference in the incoming and outgoing light where the missing intensity at certain wavelengths has been absorbed by the sample due to the light-matter interaction. The energy range of the light source and the detector determines what features will be probed by the experiment. In the UV to visible range (150-800 nm) electronic transitions between orbitals occur which gives information on the electronic structure of the molecule. The intensity of the transition is determined by the Frank-Condon factor, which is related to the wave function overlap of the vibronic wave function between both sides of the transition. In the lower energy range of IR (2,5-25 μm or 400-4000 cm^{-1}), the transitions in the vibrations of molecular bonds can be probed, this can give in-depth information about the structure of a molecular species and how it changes in a reaction. The intensity of the vibrational transitions measured depends on how they are measured. In Fourier transform infrared spectroscopy (FTIR) spectroscopy it is dependent on a change in the dipole moment of the bond, while Raman scattering is dependent on the polarizability of the bond. Overall, discrete energy levels can be described in an energy diagram, Figure 2.1.

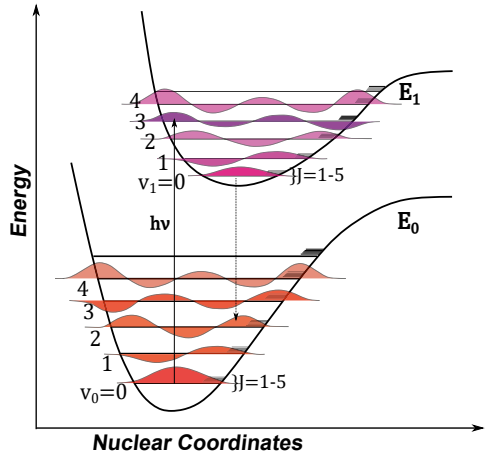

Figure 2.1. A schematic of the energy levels in a molecule, with the potential curves symbolising the electronic states E_0 and E_1, the vibrational levels V as well as their vibrational wavefunctions and on top of each vibrational level the rotational energy levels J. The arrows symbolise absorption excitation (up) as well as fluorescence emission (down).

When the energy levels go to higher energies they become closer to each other at the so-called classical limit and where the states are separated by so little energy they essentially form a continuum of states. A similar effect also happens to large chemical structures such as materials or polymers but for a different reason. The continuum arises due to the mixing of bonding orbitals forming non-degenerative energetic states, and the more bonds involved

the more possible states are available. The changes lead to the sharp absorption lines of the atoms into so-called bands which are a wider continuum of states. In semiconductors, there are energetic separations between the bands, so-called band gaps that allow for excitation between the bands. Since the number of possible states that can be involved in excitation becomes much larger than in a molecule, the bands typically allow for a wide range of excitation energies.

Other spectroscopic measurements such as photoluminescence spectroscopy utilise the emissive transitions from molecules, such as fluorescence and phosphorescence that occur as electrons relax to lower energies. Emission spectroscopy is a powerful tool to study reactions from electronically excited states as the quenching of the excited states can be used to see how other chemical processes take place. Transient techniques in the nanosecond to femtosecond ranges are also incredibly powerful tools to study how short-lived states develop over time.

2.1.2 Spectroscopy of Catalytic Mechanisms

During the types of fuel-forming reactions described in this thesis, a catalyst will undergo a range of physical and chemical transformations which will both be dictated by and change, the electronic structure of the chemical system. During a photo-catalytic process, the catalyst will first be excited, leading to a shift in electron density over the catalyst. This excited state will then go to a reduced or oxidised state as a result of electron transfer in the catalytic system, and the shift in electronic density will once again reshape the electronic structure. This state will then start to form new chemical bonds and take the structure of catalytic intermediates, and in the end, ideally, return to its initial state. The same procedure can be said for electrocatalysis with the exception that no electronic excitation takes place, instead the applied electric field will provide sufficient potential energy to start the redox event and initiate the catalytic process. However, it is also shown that the electric field itself can perturb the orbital structure of molecules inside, it a phenomenon called the Stark effect [47, 105]. This effect will shift the vibrational modes to lower energies and broaden the vibrational bands that can be seen in FTIR or Raman measurements. The presence of a strong electric field can therefore also change the catalytic properties of molecular species inside of it, something that has been recently shown to be an important factor in heterogeneous electrocatalysis [47, 48].

To probe these reactions one can use either transient pump-probe experiments where the reactions are triggered by a light pulse and then probed by

a following light probe to see how the reaction takers place. An alternative that is used in this thesis is spectro-electro chemistry (SEC) where the reactions are triggered through electrochemical methods and that is then coupled to transient spectroscopy.

2.1.3 Magnetic Resonance Spectroscopy

Not all information on the structure of a molecule is probed by looking at the electrons, rich information on the construction of a molecule can be attained by looking at spin resonances between the nuclei of the atoms [106, 107]. These techniques use induced magnetic fields to look at how strong the response of the species is. For nuclear magnetic resonance (NMR) spectroscopy the interactions between the nuclei can be measured. This gives chemical shifts that can be used to determine the molecular structure. A similar technique can also be used for unpaired electrons, electron paramagnetic resonance (EPR), and the coupling of unpaired electrons in paramagnetic species can be measured. This can be used to detect radical species and see how these unpaired electrons couple to the surroundings to determine where they are located in the structure.

In this thesis, a wide range of these spectroscopic techniques have been adapted in order to understand and describe the intermediates that arise in the catalytic systems that have been investigated. The species that have been identified spectroscopically have also been compared to species generated through quantum calculations by collaborating groups.

2.2 Chemical Environment

While the electronic structure and properties are of key importance, a catalytic mechanism is never solely reliant on the catalyst, instead, it depends on the properties of the overall chemical environment. I define the chemical environment as everything in the catalytic process surroundings such as solvents, temperature, pH, concentrations, additives, surfaces, and other boundaries. In essence, it is everything in the system outside of the catalytic site itself and fully determines the thermodynamics and kinetic limitations.

A well-functioning catalytic system needs to be well-aligned thermodynamically so that the charges will move in the correct direction with as little extra energy required as possible, in electrocatalysis, this extra energy is referred to as the overpotential. It is also important to have no significant side reactions take place. It also needs to have sufficient access to the reactants so that the system will not be limited by mass transport to the active sites.

The chemical environment can also change what type of reaction the catalyst promotes. Many catalysts can perform different reactions depending on the parameters of the chemical environment are. A basic pH would for example need the HER mechanism to swap from using free protons from H_3O^+ to a water dissociation mechanism, not something all HER catalysts can do. In this condition, the catalyst can then be used for other reduction reactions such as, for example, the CO_2RR shown later in this thesis.

2.3 Electrochemical Analysis

Since the key to all of the fuel-forming reactions is the movement of electrons, it is essential to understand the redox behaviour of both the catalyst on its own and the overall catalytic system. Perhaps the most powerful way of probing these behaviours is by using analytical electrochemistry, with the most widely used variation and often most information-rich being cyclic voltammetry. The general setup for an analytic electrochemical experiment is to use a three-electrode setup (Figure 2.2), including a working electrode (WE) where the reaction of interest will take place, secondly, a counter electrode (CE) where the charge neutralising opposite redox reaction will take place. And finally, a reference electrode (RE) against which the potential will apply, at this electrode a know redox reaction takes place to keep the reference potential steady during the full experiment. Connected to these electrodes is typically a potentiostat which allows for control of both the current and the potential that is running in the system, depending on what type of experiment is set up.

In the solution, there needs to be a significant amount of supporting electrolyte to make sure resistances a low enough to generate current and to stop

the migration of charged species. The choice of electrolyte is typically something that is very chemically stable and that will not interfere with the reaction. However, in water buffers can be used as the electrolyte that will also fill the purpose of regulating the pH of the solution. The presence of ions will lead to the formation of an electrical double layer that will both impact the surface of the electrode and lead to a capacitive background current of the electrochemical measurement. For homogeneous samples, the electron transfer will almost exclusively be outer sphere so the double layer will not impact the chemistry of the chemical reactions studied.

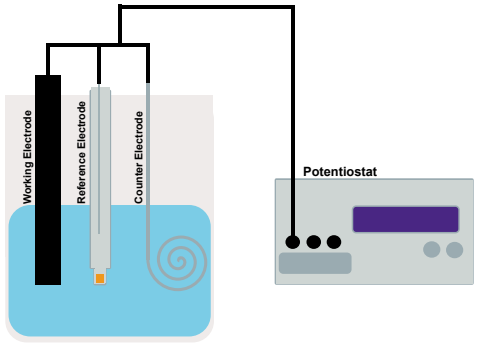

Figure 2.2. Cartoon displaying the typical setup used for analytical electrochemistry.

2.3.1 Cyclic Voltammetry

One of the most utilised and powerful techniques based on this concept is cyclic voltammetry (CV), a non-destructive measurement, where a potential is scanned back and forth in a potential range while the current is measured at the WE as a function of the potential. This means that when the potential is reached for a specific redox reaction a current will be measured at the electrode and when the potential scan reverses the opposite redox reaction can be probed [108]. In essence, this follows the simple expression of the equation 2.4, in a time frame where both species A and B are electrochemically stable.

$$A + e^{-} \rightleftharpoons B \tag{2.4}$$

The majority of CV experiments are performed without any applied convection so that diffusion is the only source of mass transport in the system, this leads to more involved data experimental analysis but also leads to incredibly information-rich data sets. The fact that mass transport is controlled by such a slow process and that the current measured is proportional to how many redox events are available leads to a peak-shaped behaviour to the current response as the diffusion layer of the redox active species is depleted [108, 109], Figure 2.3. The current response is also dependent on the scan rate ν, measured in

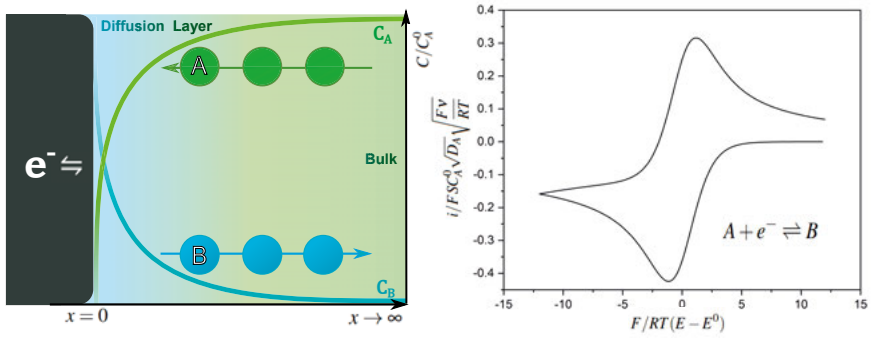

Figure 2.3. Scheme of the diffusion behaviour of the simple redox reaction $A + e^- \rightleftharpoons B$ (right) as well as a simulation of a CV for the same reaction displaying the peak shaped behaviour arising from the diffusion control (left).

Vs^{-1}, which will determine the width of the diffusion layer and in turn the current response as a faster scan rate means a stronger polarization at the electrode surface. Since the mass transport of the species is completely controlled by diffusion the expression for the movement is Fick's second law [110], eq 2.5, where D is the diffusion coefficient for species A and x is the distance of movement in absolute movement travelled in the time frame.

$$\frac{\delta C_A}{\delta t} = D\frac{\delta^2 C_A}{\delta x^2} \tag{2.5}$$

The current measured in the experiment is in turn described by Faraday's law of electrolysis that can be expressed as [111, 112], eq 2.6, where S is the surface area if the cathodic current is defined as negative.

$$i = FS\frac{\delta C_A}{\delta t}\bigg|_{x=0} = -FS\frac{\delta C_B}{\delta t}\bigg|_{x=0} \tag{2.6}$$

When inserting the law of the mass transport behaviour in the expression for the current we get the overall description for the current measured in the CV experiment, eq 2.7.

$$i = -FSD_A\frac{\delta C_A}{\delta t}\bigg|_{x=0} = FSD_B\frac{\delta C_B}{\delta t}\bigg|_{x=0} \tag{2.7}$$

From this equation it is made clear that the current is mainly dependent on the concentration gradient close to the electrode surface, this gradient, seen in Figure **??**, also determines the diffusion layer in the system. This means that the peak current coincides with the steepest point in the concentration gradient and then starts to decrease as the species starts to deplete. At what potential the current will start depends on the thermodynamic reduction potential, E^0, for the redox couple in question and is then described by Nernst's equation, eq 2.8, where n is the number of electrons transferred in the redox reaction.

$$E = E^0 + \frac{RT}{nF} \ln \frac{(C_A)_{x=0}}{(C_B)_{x=0}} \tag{2.8}$$

When a flat electrode is used, the motion of the diffusion can be simplified down to a single dimension along an x-axis where $x = 0$ at the electrode surface as notated in eq 2.6-2.8, the boundary conditions for the concentration gradient can then be set up with a semi-infinite approximation of the bulk solution which is fine in most cases due to the narrow range of the diffusion layer [108, 113]. This boundary then takes the form of:

$$\begin{aligned} &t = 0,\ \forall x,\ C_A(x,0) = C_A^0 \\ &C_B(x,0) = 0 \\ &t > 0,\ \lim_{x\to\infty},\ C_A(x,t) = C_A^0 \\ &\forall x,\ \forall t,\ C_A(x,t) + C_B(x,t) = C_A^0 \end{aligned} \tag{2.9}$$

The dependable behaviour of diffusion and the concentration gradients it sets up allows for simple mathematical descriptions for a reversible redox system where both peak current, i_p eq 2.10, and peak positions, E_p eq 2.11 are predictable quantities [108].

$$i_p = 0.446FSC_A^0\sqrt{D_A}\sqrt{\frac{nF\nu}{RT}} \tag{2.10}$$

$$E_p = E^0 - 1.11\frac{RT}{nF} \tag{2.11}$$

These parameters can also be utilized to check the ideality of the system, in the ideal case a peak split, δE_p, will be the $2.22nF/RT$ which comes out as $59/n$ mV (at 25^oC) and the current will be $i \propto \sqrt{\nu}$ if it follows Fickian diffusion.

2.3.2 Coupled and Catalytic Reactions

However, for catalytic reactions, the real power of voltammetry reveals itself in the move from simple redox reactions to coupled reactions where the electron transfer is coupled to chemical transformations. The reaction mechanisms can be separated into two types of steps electrochemical steps (E in reaction mechanisms) where a redox reaction with the electrode takes place and chemical steps (C in reaction mechanisms) where chemical steps take place unrelated to the electrode [109]. The most simple coupled reactions are either the CE reaction where a reaction first occurs in solution which makes a new redox

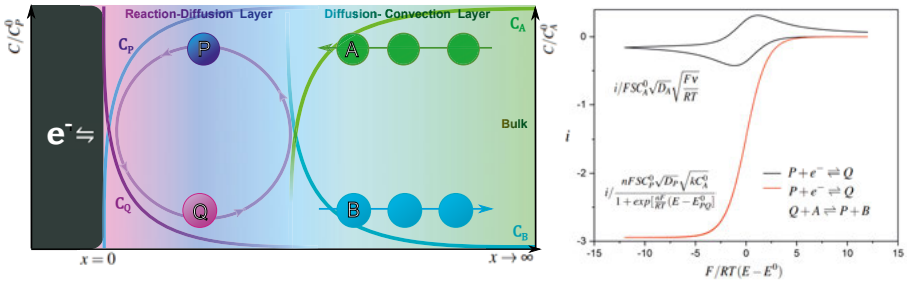

Figure 2.4. Scheme of the diffusion behaviour and concentration gradients in an electro-catalytic system following the reaction schemes $P + e^- \rightleftharpoons Q$, *and* $Q + A \rightleftharpoons P + B$ (left) and the simulation of the full catalytic CV as well as the corresponding CV without a catalytic substrate (right).

transfer possible, or the, in this context, more interesting EC reaction where a redox reaction triggers a chemical with the newly formed species. An example of how an EC mechanism can be described follows in 2.12.

$$\begin{aligned} A + e^- &\rightleftharpoons B \\ B &\rightleftharpoons C \end{aligned} \tag{2.12}$$

The EC reaction also has a characteristic behaviour in the CV where the current wave will change due to the depletion of species B. This will both lower the reversibility of the reaction depending on the equilibrium between B and C, the wave will also move to lower potentials due to the shift in the $\ln \frac{(C_A)_{x=0}}{(C_B)_{x=0}}$ ratio in 2.8. Due to the depletion of certain species in the coupled reactions the concentration gradients of the species follow different behaviours dependent on the reversibility of the chemical steps [114].

When it comes to introducing an electro-catalyst into the system an additional species, P, that will work as a redox mediator while reacting with the catalytic substrates to then turn over and return to the initial state, the simplest variation of this reaction is written as 2.13 [115, 116]. The concentration graph shown in Figure 2.4 is now replaced with the catalytic equivalent [117].

$$\begin{aligned} P + e^- &\rightleftharpoons Q \\ Q + A &\rightleftharpoons P + B \end{aligned} \tag{2.13}$$

In the ideal case, this means that the current no longer takes a peak shape but is instead sigmoidal shaped and limited by the diffusion of A, the catalytic

substrate, and will reach a current plateau with the expressions eq 2.14 and 2.15 [116].

$$i = \frac{nFSC_P^0\sqrt{D_P}\sqrt{kC_A^0}}{1+exp[\frac{nF}{RT}(E-E_{PQ}^0]} \tag{2.14}$$

$$i_{pl} = nFSC_P^0\sqrt{D_P}\sqrt{kC_A^0} \tag{2.15}$$

This ideal case is, however, rare and will be distorted by slow catalyst kinetics, substrate limitation or too fast scan rates. There are multiple forms that the wave in the CV can take depending on the limiting factors in the system, this can be used to divide the behaviour into a so-called kinetic zone diagram[118–120], as seen in Figure 2.5. For catalysts with slower kinetics, the wave will most often look something like the K zone in pure kinetic conditions where there is still a peak shape to the wave due to the consumption of the catalytic substrate. Usually, these parameters can be experimentally varied to gain more information about the system.

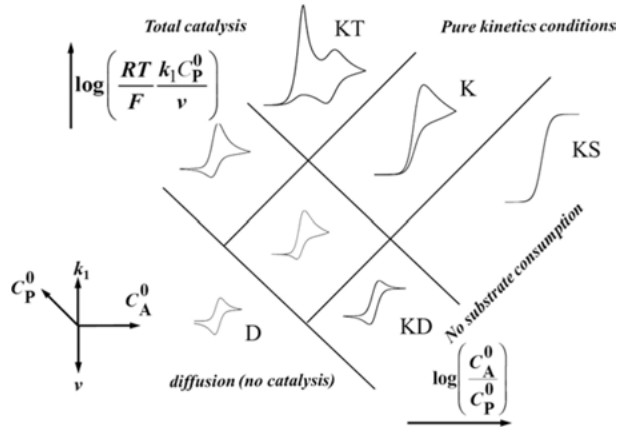

Figure 2.5. The kinetic zone diagram for an electrocatalytic system shows how the concentration ratio, the catalytic kinetics, and the scan rate controls how the current wave in a CV will look. Recreated from [120] with permissions from ACS.

For most catalysts the mechanism is not so simplistic that it can be reduced to this ideal model especially because these fuel-forming reactions require multiple charge transfers and bond formations [121]. Often all of the catalytic steps do not occur at a single potential but there can be several pre-catalytic transformations that form the real catalyst [122]. These irreversible steps that will be part of the catalytic mechanism can also be probed by varying certain parameters and see how the potential peaks react with this variation [109, 123]. A great example of this is to de-convolute what happens when the

Table 2.1. *A table showing the characteristic descriptions of different coupled EC mechanisms and the behaviour on their peak potentials when varying scan rate and concentration, including radical-radical dimerization (RRD) and radical-substrate dimerization (RSD) mechanisms.*

Mechanism	$\frac{\delta E_p}{\delta \nu}^a$	$\frac{\delta E_p}{\delta C^0}^a$	$E_p - E^0$
EC	-29.6	0.0	$-0.780\frac{RT}{F} + \frac{RT}{F}\ln(\frac{RT}{F}\frac{k_+}{\nu})$
ECE	-29.6	0.0	$-0.780\frac{RT}{F} + \frac{RT}{2F}\ln(\frac{RT}{F}\frac{k}{\nu})$
DISP	-29.6	0.0	$-0.780\frac{RT}{F} + \frac{RT}{2F}\ln(\frac{RT}{2F}\frac{k}{\nu})$
RRD	-19.7	19.7	$-0.903\frac{RT}{F} + \frac{RT}{3F}\ln(\frac{4RT}{3F}\frac{k_d C^0}{\nu})$
RSD-ECE	-29.6	29.6	$-1.15\frac{RT}{F} + \frac{RT}{2F}\ln(\frac{4RT}{F}\frac{k_d C^0}{\nu})$
RSD-DISP1	-29.6	29.6	$-1.15\frac{RT}{F} + \frac{RT}{2F}\ln(\frac{2RT}{F}\frac{k_d C^0}{\nu})$
RSD-DISP2	-19.7	39.4	$-1.14\frac{RT}{F} + \frac{RT}{3F}\ln(\frac{4RT}{3F}\frac{K_d k_d C^0 2}{\nu})$

current of a current peak increases without reaching catalytic currents, often a doubling of current. This mechanism can be a dimerization a non-catalytic ECE reaction or a disproportionation mechanism where electrons are transferred between species in the solution, refered to as a DISP mechanism [109, 124].

Some of these mechanisms are difficult to separate experimentally even with the linear fits and approximations, so more tools are needed to separate them. Due to the straightforward mathematical treatments of every single mechanistic step, simulations of CVs can be an incredibly powerful tool for mechanistic analysis. In a comparison between the ECE and the DISP mechanism, the mechanistic descriptions follows:

$$
\begin{array}{ll}
A + e^- \rightleftharpoons B & \\
B \xrightarrow{k} C & \\
\hline
\text{ECE} & \text{DISP} \\
C + e^- \rightleftharpoons D & B + C \xrightarrow{k_D} A + D
\end{array}
\tag{2.16}
$$

where the final steps can be mathematically distinguished by a simulated fit to the data.

Electrochemical methods are excellent tools to understand the thermodynamics, kinetics and mechanisms in redox reactions. They do, however, not give any information on the structure of the species that form in the reactions. So to gain a more complete understanding of what is happening, the electro-

chemistry has to be coupled to spectroscopic methods leading to the methods that are aptly called, spectro-electro chemistry.

2.4 Spectro-Electro Chemistry

SEC encompasses a wide arrangement of different techniques, essentially any combination of electrochemistry and spectroscopy can be classified as SEC. The ability to probe how the structure of a catalyst changes is of key importance to any catalytic system as a full understanding of the system is key to being able to make it better or to learn principles that can be adapted to other systems. Since many of these species are short-lived intermediates they can not be generated in bulk and must be measured at the electrode surface where the reaction takes place. Most species will have significantly changed electronic spectra when in a different redox state, both due to the difference in available electronic states and due to the perturbation of the orbitals when the electron density changes in the species. Vibrational energies will also change due to the difference in electron density, this means that the formation of new bonds can be measured and in some cases be identified.

The most powerful variations of this combination of SEC are so-called operando measurements where the reaction at the electrode can be directly probed spectroscopically as the reaction takes place. This means that some sort of time-resolved spectroscopy needs to be utilised so that the change can be monitored directly. For many processes, this can be in the time frame of seconds, but studying faster reactions might require resolutions down to the femtosecond time scale. Typically the experiment is either performed at a set potential where a single reaction can be studied or in a scanning potential experiment where the reactions during the scan can be followed.

While SEC experiments provide a lot of information on the reaction every single experiment will have different requirements, which puts high demands on the experimental setup. It requires that the light can reach the electrode surface as the new species are formed. This also means that the electrode still allows the light to be measured after it interacts with the species at the surface, so the electrode needs to be either transparent or reflective. The electrode of choice also needs to be of a material that does not interact with the reaction that is studied, this is extra important for catalytic reactions. An example of this is a Pt-based electrode, it is a malleable material that can be formed into a transparent net that is great for transmission measurements. However, Pt is perhaps the best possible catalyst for the HER which interferes both with the reaction of other HER catalysts and with the protons that are required for most variations of CO_2RR. To avoid the reactivity the choice of the electrode is often carbon-based but good carbon-based electrodes like glassy carbon (GC)

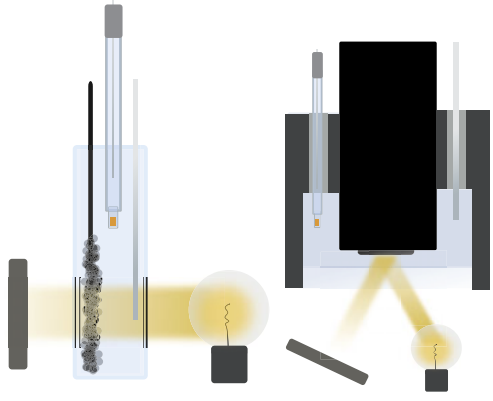

Figure 2.6. Cartoon of two SEC setups utilised in this thesis for transmission UV-Vis (left) and reflection FTIR (right).

are incredibly fragile if made to a transparent form like GC foam. While transmission measurements require specialized cuvettes, the electrodes are often easy to connect to the setup in the spectrometer. The alternative is to do reflective measurements where a normal disc electrode in theory can be used due to the reflective surface, the difficulties instead come from the fact that usually a special setup is required to couple it to most spectroscopic setups. Some examples of how the experimental setups that were utilised in this thesis can be seen in figure 2.6.

SEC is applied in most of the content of this thesis. Its usefulness in the application to understand the progression of redox chemistry, especially in combination with electrochemical analysis is difficult to match.

3. Proton Reduction and Hydrogen Evolution Centred on Benzothiadiazole (Papers I and II)

The emergence of conjugated D-A type polymers as photocatalysts led to questions rising about what the active site for catalysis is and how the catalytic mechanism works [59, 60]. Initial studies of varying the building blocks in the polymer with three components 9,9-dioctylfluorene as a donor unit and, thiophene, 2,1,3-benzothiadiazole, or a combination of the two as acceptor units [78]. In this study, it became clear that the BT unit was of key importance for the catalytic mechanism. The similar polymers F8T2, with two thiophene units as the electron acceptor, and PFBT, with BT as the acceptor, showed orders of magnitudes difference in HER activity even though their bandgaps are very similar and the energy is enough to drive the reaction. Moreover, the Pd content was similar in both polymers with F8T2 having slightly more, even so, the F8T2 systems barely showed any hydrogen evolution. Initial DFT calculations of the polymer structure also showed that the electron density was almost entirely focused on the acceptor units when the polymer was either excited or reduced. So it was clear that further investigation into BT as the active site for the HER mechanism was required.

The initial studies were focused on the polymer PFBT, however, after understanding the complexity of characterizing intermediates in the polymer the project was moved towards a different approach. No organic based HER mechanism had previously been described in these types of polymers at all and no reductive chemistry had been explored with BT as the active center. So to understand if there is a possible mechanism for catalytic hydrogen centred on BT, BTDN was chosen as the molecule of interest, a small molecule centred around the BT unit with two attached nitrile groups that would fulfil the role of blocking radical polymerization as well as be used as spectroscopic probes due to the characteristic energy of the nitrile stretching mode. In this chapter, I walk through the analysis of the catalytic pathway of proton reduction in BTDN and how these ideas can be applied in the analysis of the polymer counterparts.

3.1 The Electrochemical Behaviour of BTDN (Paper I)

The selection of BTDN as an interesting molecule to study was that the initial reduced step of a radical anion species was well studied in the literature, where the stable radical had been generated inside of micelles by photochemical methods [125–128]. This would be important since a reduction was expected to be the first intermediate in the catalytic mechanism. After a replication of this behaviour, the project was moved to focus on the electrochemical behaviour of the molecule, where the analytical depth of voltammetry could be applied. In a CV of BTDN in non-protic solvents it shows two very reversible reduction waves one at -1.06 V vs $Fc^{0/+}$ and a second at -1.88 V vs $Fc^{0/+}$.

When protons are introduced into the solution the response in the CV changes immediately with both reductions becoming irreversible and when the acid was strong enough a catalytic wave formed at the second reduction, Figure 3.1. Three acids were used in acetonitrile (AcN) acetic acid (AcA) $pK_a = 23.51$, salicylic acid (SAL) $pK_a = 16.7$, and trifluoro acetic acid (TFA) $pK_a = 12.7$ [129, 130]. Of these SAL was chosen for the rest of the studies as AcA was a too weak acid so the catalytic wave was very small while TFA was a bit too strong so the catalytic wave was difficult to distinguish from the background on a pure GC electrode. The first reduction showed a doubling of current with a slight positive shift in the potential of the wave, the slope of the potential peak change based on the $\log[\text{BTDN}]$ and $\log \nu$ showed that it was a ECE or DISP mechanism. The conclusive data was a mechanistic shift at lower concentrations around 50 μM where no current increase was observed so it fits with a EC reaction. Since an ECE reaction would not be expected to be dependent on the concentration of BTDN the mechanism was determined to be of an EC-DISP type.

The mechanism at the second reduction can be seen as a pre-catalytic formation of the catalytic species for the catalysis that happens at the second reduction. This catalytic wave was shown to be due to hydrogen evolution by measuring the H_2 content in the headspace after an electrolysis experiment. The Faradic efficiency was calculated to be 82% for two different periods of electrolysis with a TON of at least 13, with sufficiently more than that of the background with only SAL that had a fraction of the current and with only 25% Faradaic efficiency. While these are not high numbers for a HER catalyst it shows that BTDN is clearly a catalyst in these conditions and that there is a mechanism for HER centred on the BT unit.

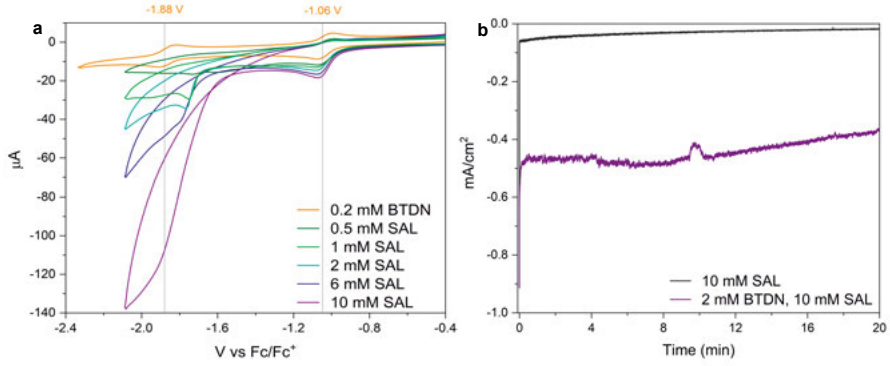

Figure 3.1. Cyclic voltammetry data of BTDN with the titration of SAL into the solution and the current from the electrolysis experiment. a) Showing how the two reversible reductions turn irreversible as more protons were added, and the doubling of current at the first reduction as well as the appearance of a catalytic wave at the second reduction. b) The currents from the bulk electrolysis experiments in AcN and 10 mM SAL, with and without 2 mM BTDN, showing how much extra current was generated with the addition of the catalyst.

3.2 Spectroscopic Insight Into the HER Mechanism (Paper I)

While the electrochemistry showed both the existence of a HER mechanism as well as some of the types of steps it goes through, it does not explain what the reaction looks like or the structure of the intermediates involved in the reaction. To understand the mechanism the intermediates were isolated and studied using an array of SEC techniques.

3.2.1 The $BTDN^{\cdot -}$ Radical Anion

Since the first step in the mechanism was an EC step it was understood that the first step of the reaction must be a reduction. This also correlates well with the fact that PFBT Pdots need an electron donor to do anything, just low pH is not enough to change anything in the system [60]. The first reduction is indeed the same radical anion species previously described from the micelle studies [126], $BTDN^{\cdot -}$ confirmed by both UV-Vis spectroscopy as well as EPR 3.2a. The EPR experiment shows a pattern of a single peak with 27 waves on it meaning it has hyperfine coupling to two chemically different nitrogen atoms which both give rise to triplets (and since $3^3 = 27$ it gives 27 peaks) which means that it is indeed a radical species and that the electron is delocalized over the entire molecule. UV-Vis spectra go from a single UV absorption at 323 nm for BTDN to at least four weaker transitions covering the majority of the visible spectra, which gives the radical solution a dark brown colour. This also makes the radical easy to identify in SEC experiments. FTIR

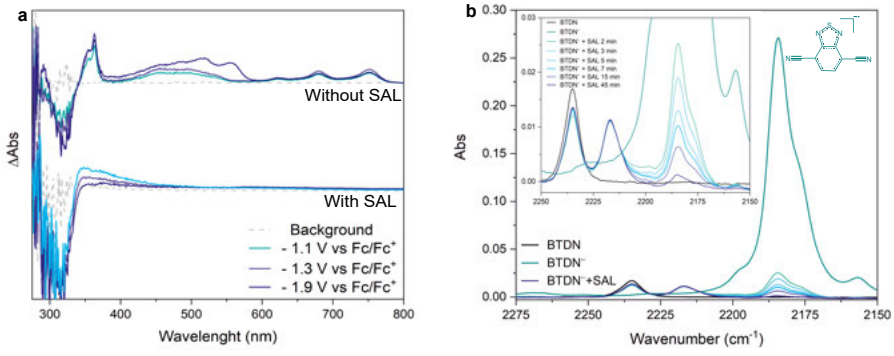

Figure 3.2. SEC of BTDN with and without an acid present. a) The UV-Vis SEC data showing the rise of the $BTDN^{\cdot -}$ radical after the first reduction and new bands corresponding to the $BTDN^{2-}$ species at the second reduction, as well as the appearance of a new band when SAL is added while all of the $BTDN^{\cdot -}$ features disappear. b) The FTIR spectra of $BTDN^{\cdot -}$ as SAL is added to the solution, following the disappearance of the 2184 cm^{-1} peak as the two new 2217 cm^{-1} and 2235 cm^{-1} peaks appear.

spectroscopy shows that the nitrile stretching mode shifts from 2235 cm^{-1} to lower wavenumbers at 2184 cm^{-1} for the radical species with a much higher absorption coefficient, Figure 3.2b. Both of these behaviours are as would be expected with a higher electron density on the BT centre. This radical anion species has also proven to be incredibly stable in inert conditions, months in an Ar glovebox, which makes it comparatively easy to study.

3.2.2 The Protonation Reaction and the Catalytic Step

The following steps after the reduction is the reaction with the acid. This reaction was probed both by mixing the radical generated through bulk electrolysis with the acid and by running SEC operando studies. In the UV-Vis operando SEC (Figure 3.2a), there is a huge difference with and without the SAL present. Without any acid the characteristic signal of the $BTDN^{\cdot -}$ rises at the first reduction and at the second reduction new spectral features can be seen, assigned to the $BTDN^{2-}$ anion that is further characterized in Paper III. When the acid is added these features disappear in favour of a shoulder feature in the first reduction that then disappears in the catalytic conditions. The disappearance of the feature is assigned to the fact that a lot of the species would turn over and BTDN would be recreated. However, it could also be that the species generated here just absorb further into the UV where both SAL and BTDN absorb and their bleach covers the spectra. According to the mechanism proposed in the next section, it seems likely that not only BTDN

is present in this condition.

In the FTIR 5 mM of the $BTDN^{\cdot -}$ radical was mixed with SAL in a 1:1 ratio, this turns out to be a pretty slow reaction so it could be studied over time in the spectrometer, Figure 3.2b. In the spectra the 2184 cm^{-1} peak can be followed as it disappears as two new features appear one at nitrile the stretching mode of BTDN at 2235 cm^{-1} and one new peak at 2217 cm^{-1} with a peak amplitude ratio of about 1:1. This could be interpreted in two ways, either that an asymmetric species is formed where the stretching modes are separated or that two new species are forming were one is the BTDN ground state species. To deconvolute these two possibilities an operando experiment was run at the conditions of the first reduction, in this experiment only the 2217 cm^{-1} peak was formed while the 2184 cm^{-1} $BTDN^{\cdot -}$ peak was still present. This concluded that the 2217 cm^{-1} peak belonged to a new symmetrical species. It was this experiment in conjunction with some good reviewer comments that led us back to investigate the mechanism of protonation to determine that it in fact was a disproportionation mechanism that occurred in the step. In fact, the $BTDNH_2$ species that is formed had previously been suggested in literature [131] and the band fits well with the value that DFT predicts.

3.2.3 The Proposed HER Mechanism of BTDN (Paper I)

From the mechanistic insights from both the CVs and the SEC, the first reaction could be determined to be the formation of the $BTDNH_2$ species from a disproportionation reaction. From the CV it was also known that this species needs to be reduced once more to lead into the catalytic step where the H_2 is released. To try and understand this step DFT calculations were applied. From these calculations, it was determined that it was unlikely that the H_2 could be released from a single $BTDNH_2{}^-$ species, however, for a hydride transfer to a proton in the solution or seemed energetically feasible. If this proton is from another of the protonated catalytic intermediates or directly from SAL was undetermined in this study but both seem possible. This mechanism leads to the end product of H_2 as well as a $BTDNH^{\cdot}$ species that would then react with another $BTDNH^{\cdot}$ in the disproportionation reaction yet again, so the full mechanism can be seen in Figure 3.3. This means that the reaction can never give a 100% Faradic efficiency, since some of the electrons will always stay in this intermediate, and the buildup of this reactive intermediate explains why the reaction can not be fully sustained. This was one of the first cases in which a HER mechanism was discovered and explained on a small organic catalyst of this kind.

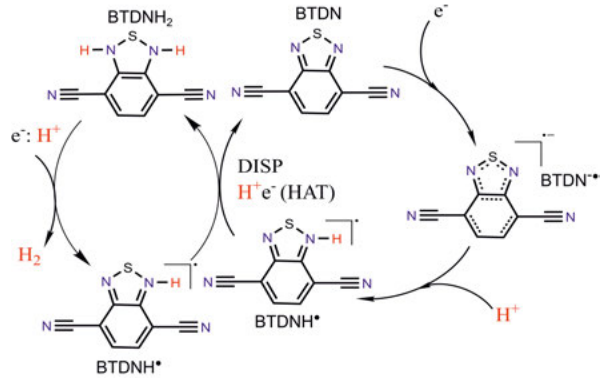

Figure 3.3. The suggested catalytic mechanism of HER from BTDN, with the generation of $BTDNH_2$ in the first reduction through the DISP mechanism and then followed by the hydrogen release after the second reduction.

3.3 The Electrochemical Behaviour of PFBT and the Molecular Analogue BTDF (Paper II)

After demonstrating that there is a possible mechanism for HER on the BT site we moved back to the PFBT polymer and photocatalytic Pdots where the project started. The goal was to identify how the BT site in PFBT reacts with protons and try and illuminate the role of benzothiadiazole in the catalytic process of PFBT Pdots. To understand this process electrochemistry was again utilised even though it is a photocatalytic process, this was the choice because is difficult to follow exact processes occurring spectroscopically, in such a complex system.

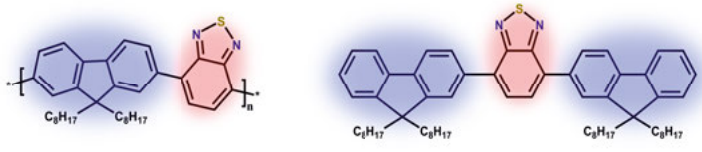

Figure 3.4. The chemical structures of PFBT and the molecular analogue BTDF.

The redox behaviour of a D-A polymer is, however, also quite complex. The electron density changes as some sites become reduced or oxidised which makes, previously identical sites now able to be reduced or oxidised at other potentials since the local environment has changed. This is clear from the CV of PFBT dissolved in THF Figure 3.5, on the scan back there are now new oxidations not directly corresponding to any previous reductions. On following scans new reductions can also be seen in the CV with varying correspondence to the new oxidative peaks. The diffusion of a polymer is also more complex

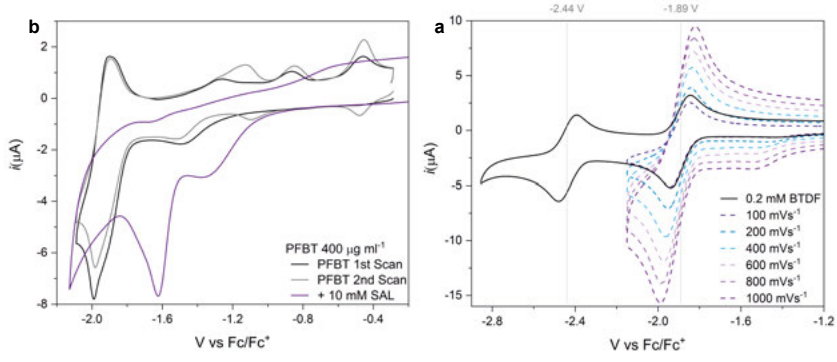

Figure 3.5. CVs of a) PFBT in the first and second scan as well as when 10 mM SAL is added and b) of BTDF at different scan rates both in THF solution

than that of a small molecule, to follow Ficks's law of diffusion a particle must follow Brownian motion and therefore be approximated as a dot or hard sphere. This is a poor approximation for a long polymer as it is better described as a string where different parts of the polymer can move in different directions at the same time. Considering this, adding acids to the CV experiment still illuminated something about the reaction. Both the visible current waves in the CV move to lower potentials as would be expected for an EC reaction and there is a large current increase in the previously very weak -1,38 vs $Fc^{0/+}$ reduction. This reaction shows that there is a reaction between the reduced PFBT and protons, but to be able to study the reaction in depth a more electrochemically well-behaved system was needed.

To emulate the BT site in the PFBT polymer the molecule 1,2,3- benzothiadiazole di-9,9-dioctylfluorene (BTDF) was synthesized. The molecule only has one BT site but is surrounded by two dioctylfluorene like it is in the polymer, however, the UV-Vis showed a similar D-A type band in the visible region although a bit blue-shifted so from the electronic structure it appears to be a good model. In the CV BTDF is, like BTDN, very well-behaved with two reversible reductions at -1.89 and -2.49 V vs $Fc^{0/+}$ and the current is proportional to the square root of the scan rate like a free diffusing molecule should be. The shift of the reductions to more reductive potentials compared to the BTDN reductions is expected since the fluorene groups are electron donating instead of electron-withdrawing like the nitrile groups are. This means that the BT centre will have a higher electron density in its ground state and therefore be more energy-demanding to put another electron there, leading to a more reductive potential. Salicylic acid was again chosen as the proton source since it had worked well for the previous study. When added to the CV experiment with BTDF clear signs of an EC reaction could be detected in the first reduction, however, since the reduction potentials required are so large no catalytic

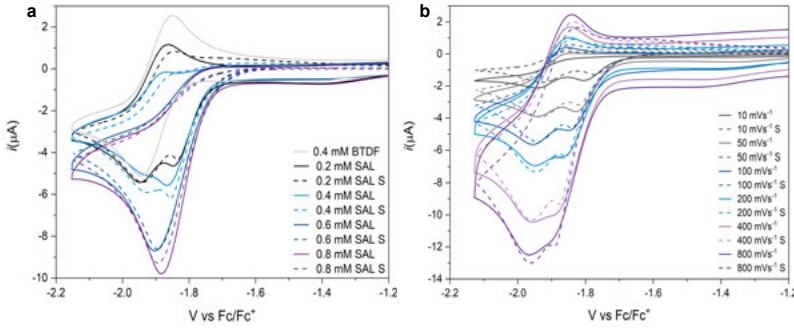

Figure 3.6. CVs and simulations (dotted lines) of BTDF in a) a titration experiment with different amounts of acid added and b) at different scan rates with a set acid concentration of 0.4mM for a 1:1 ratio.

wave could be distinguished from the background reduction of SAL on the GC electrode. The lack of a clear electrocatalytic reaction was not unexpected. It did not affect the study too much since the main goal was to understand the proton interaction at the first reduction.

To understand the proton interaction with the first reduction an acid titration experiment and a scan rate dependence experiment were run similar to the BTDN reaction in Paper I. Multiple simulations were run to understand the electrochemical reaction with different sorts of ECE and DISP combinations since the clear current doubling could be seen when at least two equivalents of acid were present. Unlike in the case of BTDN, no concentration dependence could be seen for BTDF and the fit over all the data was by far the best for an ECEC mechanism. The peak splitting behaviour is unique to the ECEC mechanism, at lower concentrations of acid only some of the BTDF will react in the ECEC way while the rest of the molecules will proceed unperturbed by the acid. So overall the same reaction takes place as for BTDN that the species would take up two electrons and two protons. However, unlike the reaction for BTDN the intermediate species was so easy to reduce (only requiring -0,5 V in the simulation) so the second reduction occurs directly at the electrode. The simulations also showed that the initial reaction between the reduced BTDF and the SAL is very fast, at least diffusion-controlled $k_r \geq 5 * 10^9$ s^{-1} M^{-1} which is important from the standpoint of electron movement in the Pdot.

3.4 Summary and Conclusions

A proton reduction mechanism centred on BT was demonstrated in all cases it was explored with a catalytic mechanism for HER found and described on the molecule BTDN, one of the first of its kind. This was also the first case where

a catalytic fuel-forming reaction has been proved on a moiety that is also a building block in D-A type polymers. In the cases where the mechanism was explored in depth, the BT seems to go to a symmetrical doubly protonated species. The electrochemical mechanism takes either the part through disproportionation or through a double reduction, photochemically the path may be different but the formation of the symmetrical species seems likely, even in this case, from an energetic point of view. The polymer PFBT will react with protons when reduced and by comparing with the model compound BTDF it seems like this is a fast process. While the catalysis from BTDN is not so impressive as an HER catalyst it shows that there is a possible mechanism centred on the BT unit.

4. Tuning Photocatalytic Reduction Processes in PFBT Pdots (Papers II and III)

In the field of polymer photocatalysts, the consensus picture has been that the residual Pd in D-A polymers is the active site for HER [54, 76, 77]. In Paper I we showed that there is a possibility for a BT-centered reaction which led us down the path to investigate what properties that control the reaction. A big difference between the studies where the Pd influence had been demonstrated and the way that our group had measured before is the conditions that the photocatalytic experiments were performed. The mechanistic studies had been performed with a 30% volume of diethyl amine (DEA) (about 0.6 M) as an electron donor while the condition that had been used in our group and by others was with 0.2 M ascorbic acid (AscA) at pH 4. Since DEA is a base with a p$K_a = 10.7$ an unbuffered solution of 30% DEA is very basic, above pH 13 [132]. So for this study, we wanted to identify how the conditions affect the catalytic activity of PFBT Pdots, including the amount of Pd in the sample and pH and look for a protonation reaction on the polymer itself as previously described in Chapter 3. In this chapter, I go through the photocatalytic reactions of PFBT Pdots and how altering the catalytic conditions alter and define the catalytic activity and what reaction takes place.

4.1 PFBT Pdots

PFBT Pdots (Figure 4.1) were prepared by nano-precipitation where a solution of the active PFBT polymer and the PS-PEG-COOH polymeric surfactant in THF, is mixed into the water which acts as an anti-solvent for the polymers. The polymers then nucleate into nano-particles as the THF evaporates from the solution to particles of around 30-100 nm depending on the polymer concentration in the THF phase. The structure of the particles is not fully understood, from microscopy it is clear that they are not crystalline as no refractive fringes can be seen but how densely packed the polymers are is still not clear. There are reports of Pdots with different morphologies seemingly dependent on the polymer and surfactant combination [133, 134]. So it is not clear what the surface area for these particles is, it seems likely that there is significant surface area inside of the particles as well as on the surface. The nature of the residual Pd is not fully clear either, according to Kosco *et al.* it is

in the form of tiny nanoparticles on the Pdot surface, but in other microscopy data, these dots are not visible. Overall the nature of Pdots being the soft matter with some micelle characteristics makes them unusually difficult to study. This is because it can not be trusted that they will keep the same morphology when dried, which is usually used to study the structure of nanoparticles.

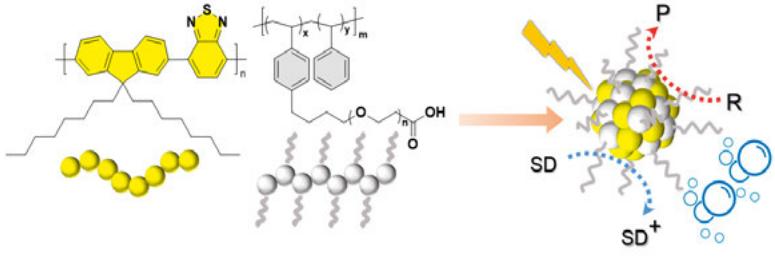

Figure 4.1. The chemical structures of PFBT and PS-PEG-COOH that construct the PFBT Pdots as well as a cartoon of the Pdots structure as stabilized by the polymer surfactant and performing the catalytic reduction reactions.

4.2 The Catalytic Activity of PFBT Pdots and the Influence of Pd and pH (Paper II)

The Pdots were prepared from two different sets of the PFBT polymer, one that was directly commercially available, and one that we had all the Pd removed from with the help of another company. The final concentrations of Pd were 1000 ppm for the commercially available one and <10 ppm for the washed one. The Pdots were made to be as similar as possible although this is not as simple as it sounds as a high variance in size, absorption, and catalytic activity can be seen even in standardized preparation conditions. However, the Pdot solutions were controlled with UV-Vis and dynamic light scattering (DLS) and kept within a few percentage variations to make sure the systems were as similar as possible. The systems were then tested in two photocatalytic conditions with 0.2 M AscA at pH 4 and with 0.2 M DEA which gives a pH of 13.5. The experiments, as seen in Figure 4.2a, showed that the pH 4 condition was by far the more efficient one while the Pd had a comparatively small positive effect on the HER. What differentiates the two conditions could be as simple as the large difference in driving force when comparing the two pH conditions, Figure 4.2b. However, it is difficult to say since the driving force for electron transfer is intrinsically tied to the SD in this type of experiment. The SDs are typically most efficient as electron donors at their pK_a so it is difficult to disentangle the effect of pH from the electron transfer charac-

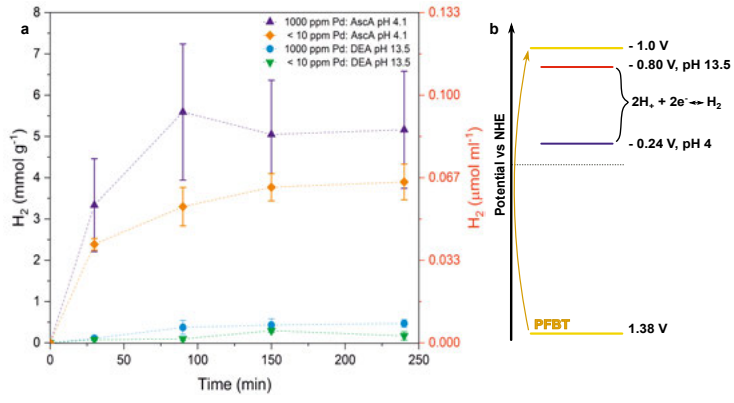

Figure 4.2. a) Showing photocatalytic HER experiments from PFBT Pdots in the different pH conditions and different Pd content. b) The driving force for the HER with PFBT Pdots at the two different pH conditions.

teristics of the SD.

To decouple the driving force for electron transfer from the pH of the solutions electrocatalytic experiments were run, something that PFBT Pdots had been shown to be capable of previously [60]. Electrocatalysis and photocatalysis are, however, not a one-to-one comparison because they differ significantly in the availability of electrons for the catalytic reaction. In a photocatalytic reaction, the initial charge separation step is the most important part of the reaction since recombination is most often the energetically most favoured path for the electron. In electrocatalysis, this is not really a problem since the electron energy is set by the applied potential so recombination becomes much less of an issue. With this said electrochemical measurements can provide a clearer picture of what does happen when the polymer is in its reduced state.

The electrochemical setup allows complete separation of the electron transfer driving force and the pH, which was required for the experiment. The pH was altered within the range of pH 4-11 by different $K_xH_yPO_4$ buffer ratios, Figure 4.3. The overall electrolyte concentration was kept to a low 0.1 M since Pdot suspensions can be destabilized by ionic strength. The CVs show a strong catalytic peak at acidic conditions, being the most active at pH 4 and then gradually dropping off to pH 7 after which the catalytic current completely drops off. The reaction was confirmed to be the HER by bubble formation at slower scan rates. The explanation for the quick drop-off in current between pH 7 and 8 is explained by the pK_a of KH_2PO_4 at 7.2. This is assigned to the possibility that when species is depleted there is no longer a strong enough acid in the solution to react with the reduced PFBT in the Pdot. This would mean that PFBT can not catalyse HER by water dissociation which explains the poor

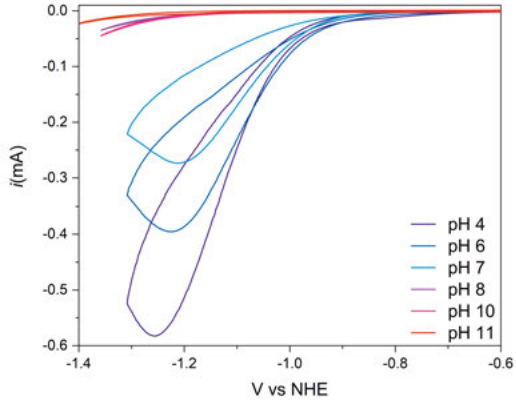

Figure 4.3. The CVs of PFBT Pdots at different pH values, display their catalytic dependence, with the catalytic wave gradually getting lower from pH 4 to pH 7 and then completely disappearing at pH 8 and higher.

photocatalytic HER from the basic solutions.

4.3 Tracking the Photocatalytic Electron Pathway (Paper II)

For the electrocatalytic experiments to make sense, an assumption is made that excited PFBT undergoes reductive quenching with the SD after excitation. There is evidence from Sachs *et al.* that the major quenching pathway in the DEA conditions is oxidative quenching by the Pd followed by electron transfer from the SD [77]. Reductive quenching with the DEA was also seen in this study, although weaker than oxidative quenching. Reductive quenching of the PFBT with AscA has also been seen both in water solutions and, in this project, in a THF solution. So it might be the case that both reductive pathways take place but it seems that the reductive pathway should be dominant when the Pd concentration is as low as <10 ppm, since the likelihood of a nearby Pd centre is very low.

In their study, Wang *et al.* noticed that adding the fullerene electron acceptor, phenyl-C61-butyric acid methyl ester (PCBM), to the Pdots completely stopped the HER from the Pdots in a pH range from 0-14 [135]. Interestingly, when reduced the energy of this compound should still be enough to perform the HER especially if the electron first reduced Pd. Still, no catalytic performance was seen even at pH 0. However, these experiments were per-

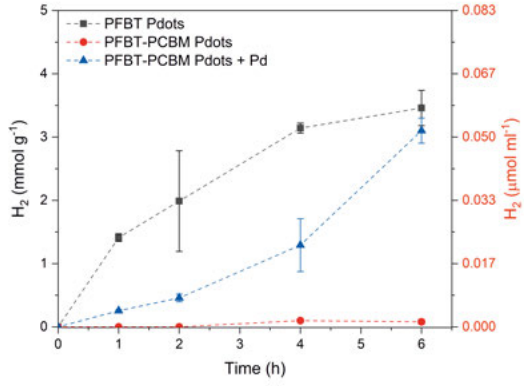

Figure 4.4. The photocatalytic experiment of PFBT Pdots with and without the addition of the PCBM acceptor, also shows that even with a significant addition of 5 w% Pd the catalytic activity is barely recovered.

formed with methanol as the electron donor so we performed the experiments again with AscA as the SD. In these new experiments (Figure 4.4), we saw the same result, the HER was almost completely quenched compared to the Pdots without the PCBM and substantial amounts of Pd or Pt needed to be added as co-catalysts to the Pdots to regain the catalytic activity.

In the same study, they showed that the electron transfer between PFBT and PCBM was very fast around 400 ps so in this case oxidative quenching would be the kinetically dominant electron pathway. This also means that no significant amount of reduced PFBT would have the chance to form. A reduction in the driving force by electron transfer to PCBM would only be expected to lower the catalytic efficiency, not quench it completely, one might even expect an increase in catalytic efficiency due to the improved charge separation. The complete lack of any catalysis when the PFBT is not reduced makes it seem likely that this is an important catalytic intermediate. Bringing this together with the fact that reduced PFBT will react with acidic protons in the solution at a seemingly high rate, as shown in the electrochemical data with PFBT and BTDF in Chapter 3, it seems that the protonated PFBT species would also be a catalytic intermediate. The nature of the catalytic site is, however, still not fully determined. It is difficult to fully rule out Pd as a catalytic centre, and it more than likely contributes to the catalytic activity even if the majority of the activity would occur on the polymer backbone. If the Pd is the only catalytic site it is very efficient since it is highly catalytically active even at a concentration of <10 ppm. In this case, it also seems likely that the polymer is very good at moving both electrons and protons to the active site since the protonated BT site seems important to the catalytic activity.

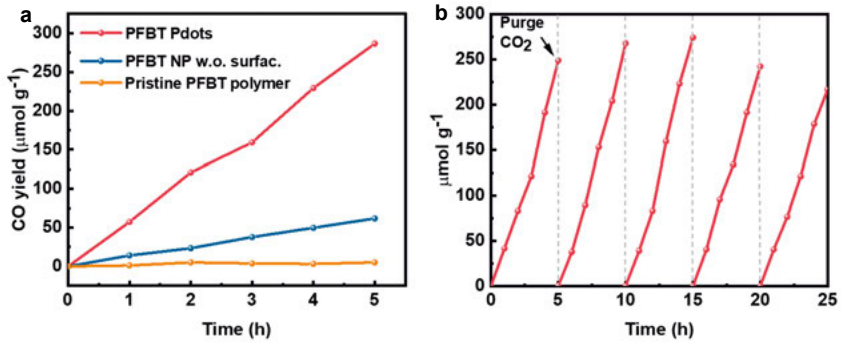

Figure 4.5. The photocatalytic activity for CO evolution, a) by PFBT in three forms of suspensions with 0.2 M TEOA and b) Pdots where CO_2 is readded into the system every 5 hours.

4.4 Switching the Reaction to CO_2 Reduction (Paper III)

The insight that the HER process in PFBT Pdots could be more or less turned off by moving to basic conditions in Paper II, in combination with that we had seen an interaction between BT and CO_2 in electrochemistry (discussed further in Chapter 5) led us to investigate if we could change the catalytic process from HER to the CO_2RR. To achieve this it is clear that a SD that is active in basic conditions was required, three SDs were tried ascorbate (NaAsc), triethylamine (TEA), and triethanolamine (TEOA). NaAsc turned out to be inefficient due to the low pH in which it operates so the HER was still a problem and TEA while basic did turn out to not be as efficient. So in the end, the SD of choice was TEOA which has a pK_a of 7.9 but works best in pH ranges above pH 8 due to its decomposition pathway [68]. TEOA can also function as a proton source when it has been oxidised which is needed for an efficient CO_2RR reaction, this is likely why it is more efficient than TEA for this purpose. The 0.2 M TEOA solution gives a pH of around 10 so it is both basic enough to stop the HER and to keep TEOA in its optimal condition as a SD.

The Pdot solution was saturated with, and put under a CO_2 atmosphere by flushing the solution vial with CO_2 gas for half an hour. In this condition, we could indeed, see a photocatalytic reduction of CO_2 to CO at a rate of 57 $\mu Mg^{-1}h^{-1}$, Figure 4.5. This reaction was also shown to be significantly enhanced by the Pdot structure when compared to Pdots without the PS-PEG-COOH surfactant or pristine PFBT powder. This behaviour leads credence to the idea that the morphology of the Pdots is not completely closed but has a porous character where the reaction can take place inside of the particle and not just on the outer surface. The CO was confirmed to come from the CO_2

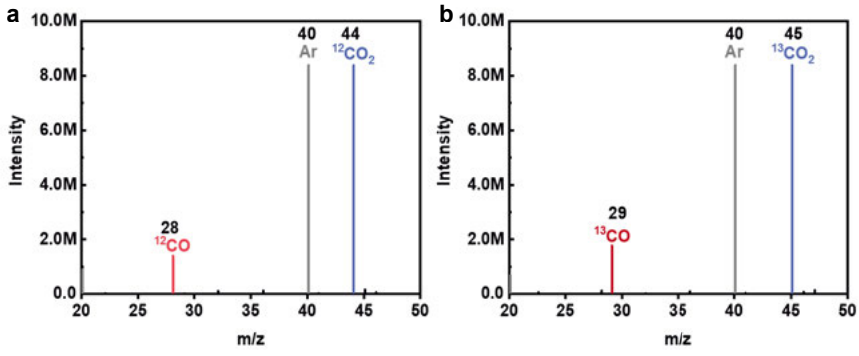

Figure 4.6. The isotopic Co evolution experiments, displaying that depending on the CO_2 gas different isotopes of CO will be generated.

gas and not from any other source by isotope experiments where $^{13}CO_2$ gas was used, Figure 4.6. In these experiments exclusively ^{13}CO was produced instead of only ^{12}CO in the experiments with the regular $^{12}CO_2$ gas. Moreover, no other carbon-based product was detected in NMR experiments which makes it seem that the selectivity towards CO conversion is high, although it can be difficult to detect all possible CO_2RR products, this is discussed further in Chapter 5.

From quenching experiments in Figure 4.7, it can be seen that the fluorescence lifetime is not quenched noticeably by only the CO_2 but it is by the TEOA SD. This shows that the particle likely goes through reductive quenching as the first step in this reaction as well. For the reaction mechanism, the influence of Pd was tested here as well, since Pd is a known catalytic site for the CO_2RR from CO_2 to CO [136]. However, neither the removal of Pd by washing it nor the addition of more Pd seemed to have a substantial effect on the catalytic activity. This indicates that the most important factor for catalysis is centred on the polymer backbone, similar to the HER. The mechanism was investigated using electrochemistry, SEC, and DFT calculations and is further discussed in Chapter 5.

Unlike the acidic HER condition, where the catalysis is only stable for a couple of hours, the catalytic activity could also be maintained for 25 hours by purging the solution with CO_2 every fifth hour. This could either be due to the stability of the particle suspension, it has been seen that aggregation leads to reduced catalytic activity, or it could be due to chemical or photochemical degradation of the catalyst. Often photo-degradation is attributed to charge accumulation or oxidative stress from oxygen species [137]. But in the case of polymer-centred catalysis, it could also be due to the buildup of unstable catalytic intermediates or alternative routes to the catalysis where the species

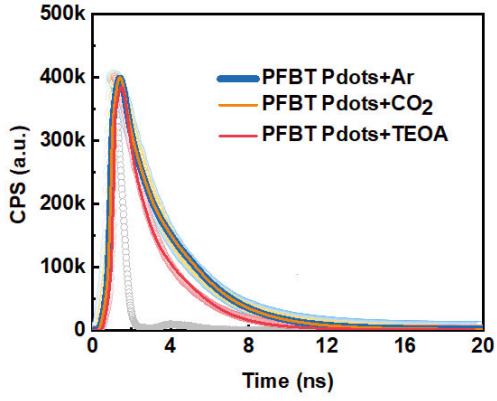

Figure 4.7. The fluorescence quenching experiments show the quenching from TEOA but no significant quenching from CO_2.

are more stable. This is also a possible problem of having polymer-centred catalytic reactions if the goal is only to use the polymer as a photosensitiser the chemical reactions centered on the polymer can be problematic. However, if the goal is to have a fully organic catalyst then it is important to be able to understand the chemical mechanism that occurs on the polymer itself.

4.5 Summary and Conclusions

We have shown that tuning the reactive conditions of PFBT Pdots has a large effect on the catalytic performance of the particles and what catalytic mechanisms they can access. The pH is very important for any reaction that includes protons and can dictate the availability of an HER mechanism which is important depending on the target reaction. For both the reactions investigated it seems that the influence of Pd is low, while the availability of reduced polymer is very important. The choice of polymer system is, therefore, more complicated than just selecting a good light absorber with good photo-physical properties, the chemical reactions that can take place on the polymer also need to be considered. These reactions can be helpful if the system will work catalytically on its own, without a co-catalyst, and might be lowering the catalytic output if the polymer is only there to be an electron mediator to an active catalyst. The particle structure also seems like a key parameter either through the available high surface area or due to possible active sites inside of the particle.

5. Reduction and Capture of CO_2 with Benzothiadiazole Centered Systems (Papers III and IV)

The idea of fully organic CO_2RR electrocatalysts has been around for a while with the first report of the pyridinium ion seemingly being able to convert CO_2 into methanol with an impressive Faradic efficiency of 20% [138]. However, this has turned out to be a pyridinium-assisted mechanism requiring a catalytically active electrode surface to actually perform the catalysis [139, 140]. This surface-mediated technique has since been worked on [100, 101, 141, 142], but aside from the hydride systems described in the introduction and a variety of organic materials [143–147]. There are few examples of small molecules performing the reaction on their own without the hydride mechanism one example is triazole which has been reported to reduce CO_2 to formic acid by only the surface energy of micro-droplets [148].

Another important reaction for the energy transition and reducing the environmental impact of the pollution that has been, and will be produced, is CO_2 capture [149]. This could be done in a magnitude of different ways some physical and some chemical and some a combination of both. One method to do this is by using molecular redox carriers that can bind the CO_2 electrochemically [150]. Recently BT was shown to be able to perform such a reduction in a two-electron reduction which is followed by the binding of two CO_2 molecules in the process [151]. Simultaneously, we have been working on the same reactions yet again based on BTDN and PFBT. BTDN is an interesting molecule for these reactions because it is much easier to reduce and has two reversible reduction steps in the window that BT only has a single one. In this chapter, I discuss the interactions of BTDN with CO_2 in its reduced states as well as the interaction and insight we have gotten into the CO_2 reduction mechanism of PFBT.

5.1 The Interaction Between BTDN and CO_2 (Paper IV)

This project took its start close to our discovery of BTDN as a HER catalyst where we became interested in its ability to catalyse other reduction reactions such as the CO_2RR as well. A few CV experiments showed a clear interaction between the reduced species and CO_2 from the telltale signs of a positive shift

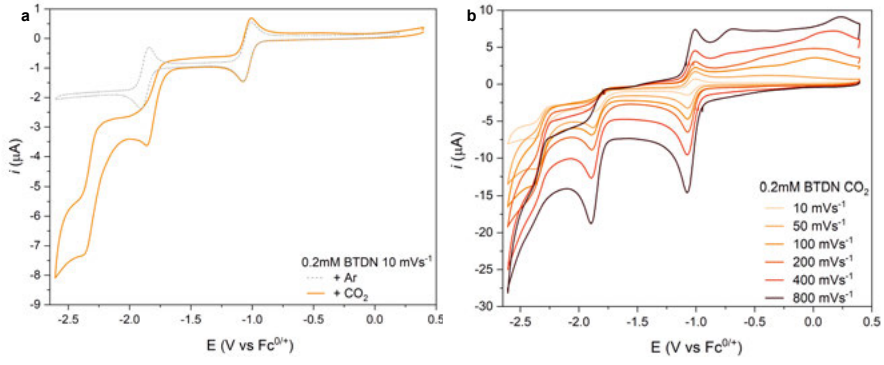

Figure 5.1. CVs of BTDN in the presence of CO_2. a) 0.2 mM BTDN with and without CO_2 in the solution at 10 mVs^{-1} b) Scan rate dependence of BTDN in saturated CO_2 solution, showing how the peak ratios shift.

in the reduction potential and an increase in current in the second reduction. Returning to the project we realized that the story is much more complex than the initial considerations with interactions between CO_2 and all of the reduced states of BTDN.

In the CVs of BTDN in a CO_2 saturated AcN solution, there are three reduction waves appearing, Figure 5.1. The first reduction looks mostly unperturbed at slow scan rates (<100 mVs^{-1}) while losing some reversibility at faster rates. The second reduction both shifts to a more positive potential and gains an increase in current so it is a clear indication of an EC mechanism coupled to a further electron transfer step ending up into something like an ECE or DISP mechanism. This reaction also shows a scan rate dependence where the current ratio as compared to the first reduction becomes lower and lower as the scan rate increases, from a ratio of above 2 at 10 mVs^{-1} to around 1.3 at 800 mVs^{-1}. The ratio above 2 could be due to the shifting background current or potentially due to several reactions occurring at the same time. The decreasing ratio is assigned to the kinetics of the reaction that takes place at this potential, slow kinetics would mean that the full reaction does not have time to take place so all the electrons do not have time to transfer which leads to a lower current. In theory, the kinetics could be extracted from this wave, by for example simulating the mechanism, however, the reaction is quite complex as demonstrated later in the chapter and if the mechanism is unknown there is no point in trying to extract any kinetics.

The third reduction that appears is something completely new that is related to the CO_2 bound species that has been formed in the second reduction. The third peak shows the largest scan rate dependency of the three because it is dependent on the species that form in the second reduction. Interestingly, at 10

Table 5.1. *Table displaying the peak currents and current ratios of the three reduction peaks with the third reduction taken at -2,4 V vs $Fc^{0/+}$, measured at different scan rates for 0,2 mM BTDN in CO_2 saturated AcN.*

ν (mVs^{-1})	i_{pR1} (μA)	i_{pR2} (μA)	i_{pR3} (μA)	i_{pR1}/i_{pR2}	i_{pR2}/i_{pR3}	i_{pR1}/i_{pR3}
10	-1.46	-3.63	-7.36	2.49	2.03	5.04
50	-3.24	-5.87	-11.48	1.81	1.96	3.54
100	-4.71	-6.86	-13.70	1.46	2.00	2.91
200	-6.48	-8.87	-14.80	1.37	1.67	2.28
400	-9.56	-12.7	-17.25	1.33	1.36	1.80
800	-14.58	-18.75	-18.44	1.29	0.98	1.26

mVs^{-1} this wave has a five times larger current than the first reduction. Since the first reduction in this measurement is basically completely unperturbed as compared to the BTDN scan in the Ar atmosphere, and that reduction was confirmed to be a 1 electron transfer in Paper I, that means that 8 electrons are transferred in the forward scan. On the reverse scan, there is only one clear oxidation peak meaning that there are 7 electrons missing in this scan. A small part of the current can be explained by the fact that there seem to be some more sluggish oxidation processes that are more clearly seen as broad oxidation peaks at potentials lower than the first reduction, at the faster scan rates.

The missing electrons show that something stable is generated during the scan and since the first reaction looks unperturbed it seems like it has left the BTDN in its initial form. From this data, it looks like a catalytic reduction process has taken place in the CV, however, as discussed later in this chapter, while so impossible products were identified, it is not quite clear were all the electrons go in this reaction. Since there should be no protons in the solution there is a very limited scope of products from the CO_2RR, though water can not be excluded as a proton source AcN should be sufficiently dried by 3Å molecular sieves after 24 hours to rule it out as a dominant proton source [152]. It is however known that CO can be formed without a proton source as another CO_2 molecule can act as an acceptor for the oxygen, forming carbonate ions (CO_3^{2-}) [153]. Another reduced species of CO_2 that can be formed without any proton is the oxalate ion ($C_2O_4^{2-}$) so both of these species were looked for in the spectroscopic parts of the project [154].

5.1.1 Detecting CO_2 Bound Species (Paper IV)

Like in Paper I the obvious next step to clear up what happens in the different reductions was to move towards SEC. When it comes to CO_2 reduction SEC with FTIR becomes even richer in information since CO_2 itself has a characteristic absorption in this range, around 2340 cm^{-1} in THF and AcN, that is

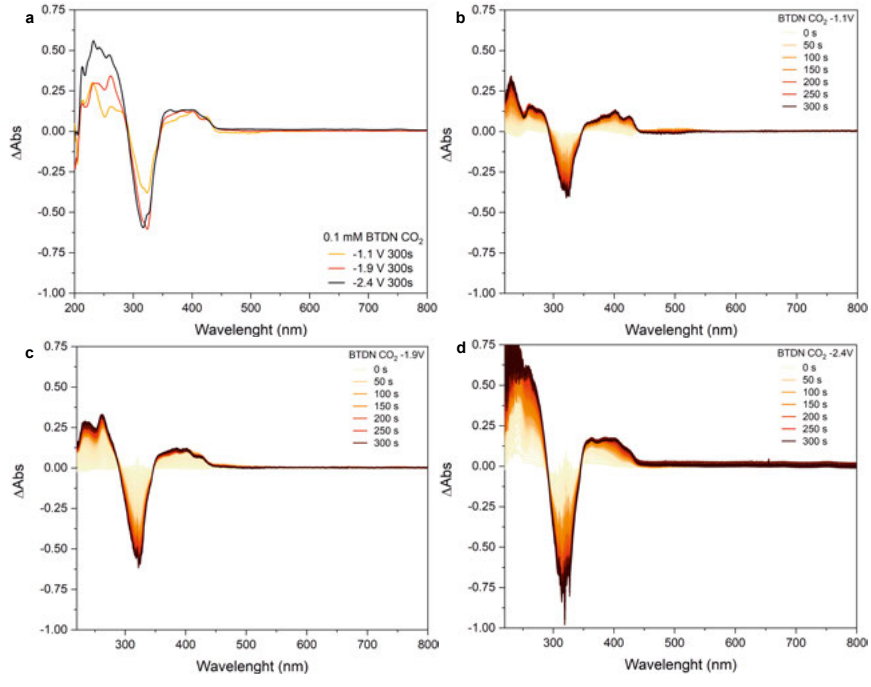

Figure 5.2. The data from the SEC UV-Vis of 0.1 mM BTDN at the three reduction potentials b), c), and d). As well as a) the comparison of the spectra of the reduced species after 300 s.

also quite different from the modes that absorb from the bound species that are more similar to carbonate or carboxylic acid bands and absorb in the, 1500-1700 cm^{-1} range.

The first experiments run were, however, UV-Vis SEC which, while not being as structurally rich can help differentiate the different species that arise during the different reductions, the spectra can be seen in Figure 5.2. The first thing that is very noticeable is the spectra in the first reduction that looks nothing like the spectra of the $BTDN^{\cdot-}$ anion as seen in Figure 3.2, even though these are the features one might expect from the unperturbed nature of the first reduction in the CVs. So the fact that the spectra look so different shows that even in the first reduction there is a reaction between the reduced BTDN and CO_2 that changes the electronic structure significantly. In the second and third reductions, there are also significant differences in the spectra especially in the 200-300 nm region and when comparing the intensities of absorption in the 350-450 nm wide bands that appear in all of the three reduction spectra.

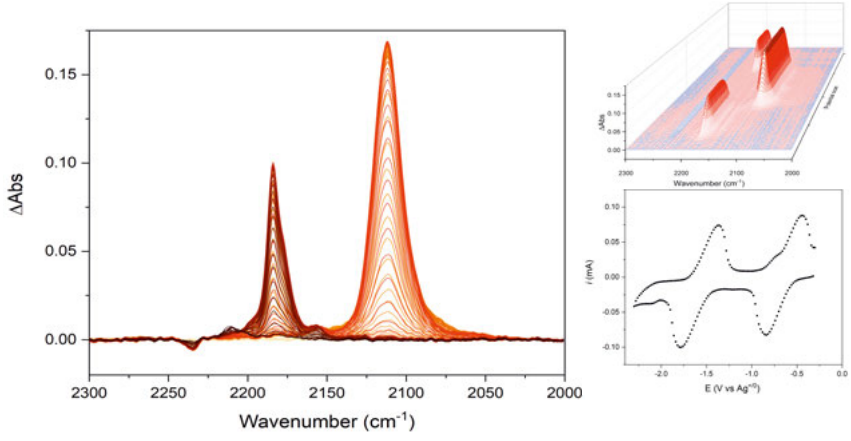

Figure 5.3. The SEC IR measurements of BTDN under Ar atmosphere, show how the nitrile stretching bands shift to lower wavenumber as the BTDN becomes more reduced, and the peaks corresponding to the two reduced species rise and fall as the CV progresses.

5.1.2 FTIR SEC to Detect Bound CO_2

When moving to FTIR SEC we used a cell where the sample was measured in a film between a glass and a GC disc electrode which the light was reflected against, as drawn in the cartoon in Figure 2.6. This setup allows for pretty well-defined CVs to be measured alongside the spectroscopic changes, which makes it easier to couple the changes to the electrochemical reactions. When measuring the SEC in an Ar atmosphere, Figure 5.3, it can be seen that both the reductions in the CV look similar to how they did in the regular electrochemical cell. The IR spectra show first an appearance of the 2184 cm^{-1} peak as seen for the $BTDN^{\cdot-}$ species in the IR SEC in Paper I. For the second reduction, the nitrile stretching band moves even further to lower wavenumbers with an even more intense peak at 2112 cm^{-1} assigned to the $BTDN^{2-}$ species. On the scan back the same reactions happen in the reverse order as expected.

When CO_2 is added to the system things become much more complex, Figure 5.4, with a wide array of peaks appearing, after the second and third reduction, in the 1500-1700 cm^{-1} range of the spectra where the bands belonging to the bound CO_2 are expected to appear. Interestingly the first reduction goes through the $BTDN^{\cdot-}$ species here and does not seem to react the behaviour is ascribed to very slow reaction kinetics between the $BTDN^{\cdot-}$ and CO_2, which is only seen in the UV-Vis SEC due to the big difference in concentration between BTDN and CO_2 in that measurement. The new peaks from the CO_2 species evolve over the CV where some peaks keep growing over the experiment while some appear at certain potentials and then disappear. In the fixed potential experiments it is clear that the peaks grow at different rates so they

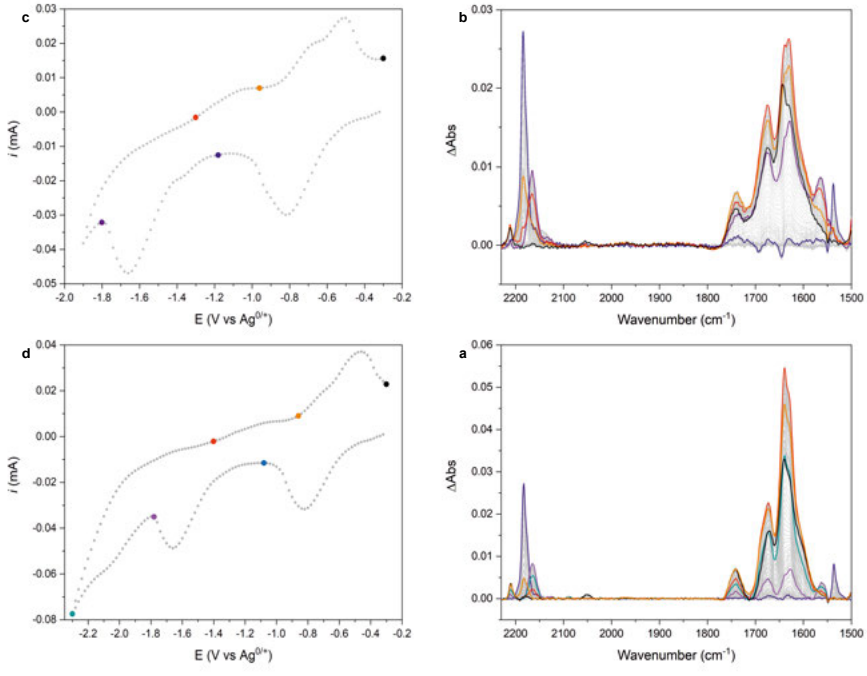

Figure 5.4. Showing the SEC IR measurements of BTDN with CO_2, with the CVs and correspondingly coloured spectra IR related to specific points in the CVs. Stopping at the second reduction (a and b) and moving to the third reduction (c and d).

do not all belong to a single species but a mixture. This makes sense from the perspective of the CV experiments where it is clear that there are multiple electrons transferred and multiple chemical steps even in just the second reduction wave. To try and figure out if some of the bands correspond to any ionic species stemming from the CO_2 we synthesised tetrabutylammonium (TBA) salts of bicarbonate (HCO_3^-), CO_3^{2-} and $C_2O_4^{2-}$. Of these salts, it seems like HCO_3^- is the most likely to be in the mixture but it could also be that some of the CO_2 bound BTDN variations have very similar peaks. In the IR SEC experiments, the peak ratio is around 1 or a bit more so it is mostly similar to the fast scan rate experiments even though the scan rate in these experiments is about 20 mVs^{-1}. The behaviour can be explained by the fact that the concentration ratio between BTDN and CO_2 is much lower in the SEC experiment since 5 mM BTDN was used compared to the 0.2 mM in the CV experiments, the diffusion is also more constrained in the SEC experiment since the measurement is done on a thin film and not in bulk solution. The restricted amount of electrons transferred in the measurement could be a reason why no clear catalytic products are seen in the data.

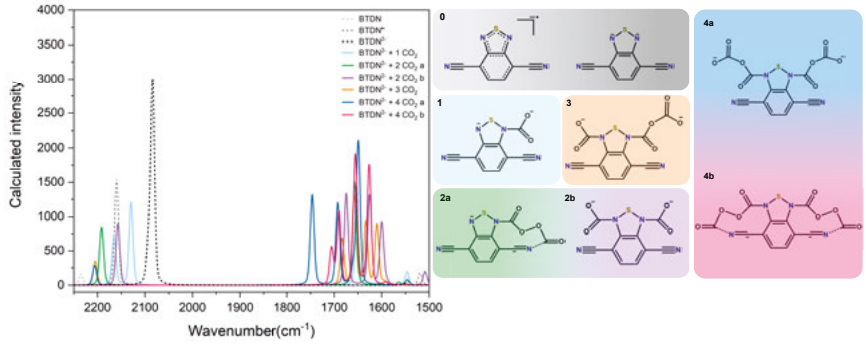

Figure 5.5. The DFT calculations of BTDN and a variety of CO_2 bound species displaying their IR absorption in the region of interest as well as their chemical structures.

To try and understand what species we were seeing in the IR spectra we did DFT calculations of many possible structures of reduced BTDN and attached CO_2 molecules. However, the DFT did not turn out to be as helpful as hoped to distinguish the arising species because it is possible to calculate a large variety of CO_2 bound species that all have bands in the 1500-1750 cm^{-1} range, Figure 5.5. By comparing the data and using the nitrile stretching bands as a reference I was able to suggest the appearance of two states in the second reduction where it seems the $BTDN^{2-}$ will first bind two CO_2 molecules to form the 2b species (Figure 5.5). The reaction then continues to bind two more CO_2 molecules to form the 4a species that seems to build up over the CV scan. The 1740 cm^{-1} band assigned to the 4a species does not grow if the potential is set for the third reduction directly in a potential step experiment, since more electrons are transferred at their potential it makes sense that either this species or an earlier species is further reduced. The species assignment is overall speculative since the bands in the DFT calculation are so close and blend together in the experimental data.

5.1.3 Catalytic Product Formation and CO_2 Release

To try and look for the formation of any catalytic products in the third reduction wave, we performed bulk electrolysis experiments at this reduction potential. From the analysis of the sample, there was still no conclusive data on the possible products. We do see tiny amounts of CO forming but only at around 1% Faradic efficiency, and while there is a band in the NMR that does look like $C_2O_4^{2-}$ and fits decently with the IR spectroscopy of the TBA salt. So it is difficult to say that BTDN is an active catalyst for the CO_2RR at least in the conditions measured, and likely most of the electrons go into binding CO_2.

The bound CO_2 was able to be released from the bound states in several different ways. For the interaction between $BTDN^{\cdot-}$ and CO_2 we could see

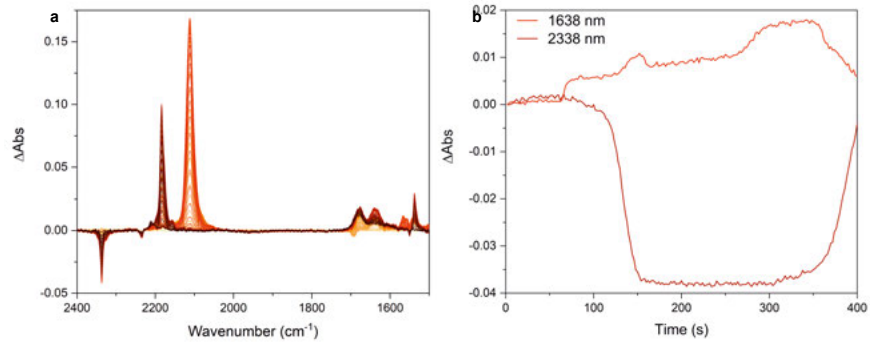

Figure 5.6. The SEC IR of BTDN in low a low Ar atmosphere a) showing the spectra as the BTDN is reduced and re-oxidised b) following the amplitude of the 2338 cm^{-1} and 1638 cm^{-1} peak over the CV cycle.

that when acid was added to the solution the $BTDNH_2$ species formed, as confirmed by IR, we could also see the concentration of CO_2 increasing in the headspace by measuring with GC. When doing SEC with a low concentration of CO_2 in the atmosphere a bleach of the 2338 cm^{-1} band belonging to CO_2 can be followed as the BTDN is reduced and on the back scan the band recovers fully, Figure 5.6. In this scan, a peak at 1638 cm^{-1} can be seen to rise and fall in the same scan, attributed to the species that captures and releases the CO_2. So it seems like the CO_2 binding is, for the most part, reversible.

5.2 Investigating the Interaction Between PFBT and CO_2 (Paper III)

To investigate the interaction between PFBT and CO_2 that leads to the photocatalytic formation of CO from Pdots. We used the same toolkit as had been successful for the studies of the BTDN interaction with CO_2. I started like usual by measuring the CV to see if there were signs of a reaction with just the polymer dissolved in THF. The CVs, Figure 5.7, show that there is clearly a reaction between CO_2 and the reduced polymer, although not a catalytic one. The reductive current slightly shifts toward less reductive potentials and is slightly increased, the biggest difference comes in the lack of any oxidative peaks where the measurement in Ar has many oxidations on the return scan.

Since this interaction is so apparent in the case of BTDN we figured that the formation of a CO_2 bound should be visible in the SEC UV-Vis experiment. Indeed we can see very clear spectral shifts when the experiment is performed under an Ar atmosphere or a CO_2 atmosphere. In the Ar experiment, the difference spectra are dominated by large bleaches by the main absorption bans of PFBT, at 450 nm and 320 nm, with some increase in absorption, mainly

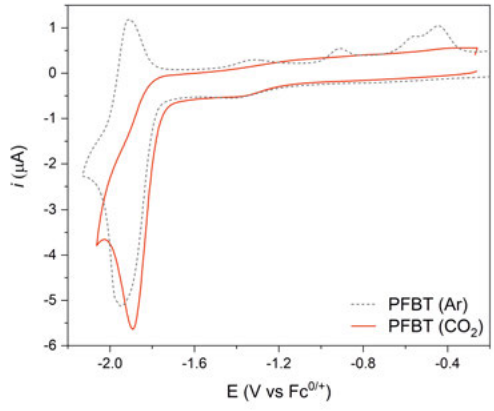

Figure 5.7. The CVs of 200 μg ml^{-1} PFBT in THF under the atmosphere of Ar and CO_2.

a wide band stretching from 500-700 nm. When CO_2 is present the bleach bands can be seen to form initially but instead of growing over the duration of the experiment, there are new absorbing bands rising. There are three new peaks forming, one strongly absorbing at 200 nm, one at 350 nm, and the third a bit wider band at 420 nm.

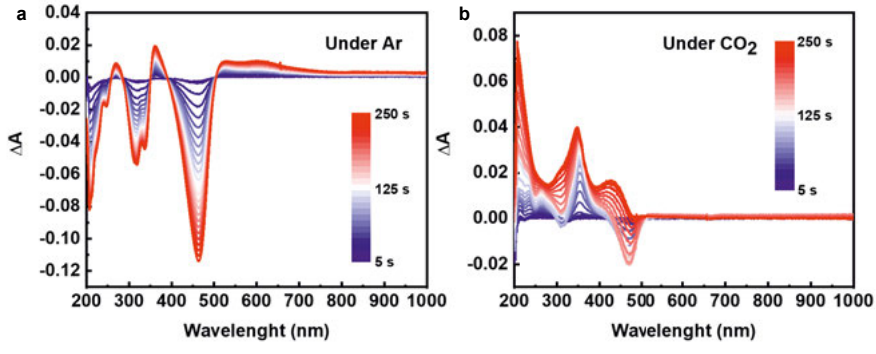

Figure 5.8. The SEC UV-Vis of 100 μg ml^{-1} PFBT in THF under the atmosphere of a) Ar and b) CO_2 in the first reduction at a bias of -2V vs Ag$0/+$ for 250 seconds.

This interaction shows that like BT and BTDN, PFBT will bind up CO_2 once reduced. However, the fact that we do not see a catalytic current hints that some more complex mechanism takes place in the Pdots. One candidate for the active site could be Pd, but as discussed in Chapter 4, neither increasing nor decreasing the Pd content significantly changes the catalytic activity of the

Pdots. So to try and understand this better we did some DFT calculations on a very simplified analogue of the PFBT polymer. These calculations show that two reduced BT sites need to be in close proximity to have a significant driving force for the release of a CO molecule. If this is true it makes sense that the polymer on its own is not catalytic because the reduced sites can repel each other in the freely solvated polymer state. In the Pdot the structure is more locked in due to the hydrophobic interactions with water, moreover, if the Pdots are indeed porous there will be channels inside of the Pdot where BT sites will be both close to the particle surface as well as other surface facing BT sites. So in these channels, a double-site mechanism makes sense.

5.3 Summary and Conclusion

We can see that BT, in all the forms that it has been studied so far, will react with CO_2 when it is reduced. In most cases, the interaction is binding of the CO_2 but there are cases where it can catalytically be released in the form of CO_2. For BTDN we can see that it will react with CO_2 at three different reduction potentials and will bind up multiple CO_2 molecules, we have also seen an increase in current that seems catalytic but have been unable to determine any products except for a tiny amount of CO. For PFBT Pdots we have shown that there is an interaction between the reduced polymer and CO_2 but for catalysis to take place it seems that the Pdot structure and possibly the chemical environment is of great importance.

6. Summary and Outlook

The understanding and advancement of the catalytic reactions involved in the generation of renewable fuels are pivotal for facilitating the transition to sustainable energy sources. One intriguing category of catalysts for such reactions comprises organic materials, which combine the adjustable characteristics of molecular catalysts with the scalability and durability seen in material catalysts. Nevertheless, our understanding of the catalytic mechanisms within these materials remains an ongoing area of investigation. Over the past decade, there has been substantial attention directed towards D-A type polymers as promising photocatalysts for fuel-forming reactions. However, the precise mechanisms underlying these reactions remain largely unexplored. This thesis focuses on elucidating the role of the molecular unit benzothiadiazole in catalyzing fuel-forming reactions within various molecules and polymers.

Papers I and II investigate the reaction mechanism of HER from BT-based systems. A seemingly general reaction between the reduced BT unit and protons is distinguished showing that the BT is likely to form a symmetrical species with protonation sites on the nitrogen atoms. Paper I shows that the small organic molecule BTDN is a catalyst for the HER, one of the first catalysts for this reaction, with this type of molecule. The catalytic intermediates were identified spectroscopically and a disproportionation mechanism could be identified by combining electrochemical and spectroscopic data. The significance of identifying catalytic intermediates on the acceptor moiety of a photocatalytic D-A polymer can not be understated. The design principles for new catalytic polymers are currently mostly focused on the energetics and photophysical properties of the polymers while the chemical properties have been more or less ignored [54, 79]. I would argue that the choice of acceptor moiety needs to be deliberately chosen depending on what role the polymer is expected to perform. If the polymer is only expected to work as a light harvester, a chemical reaction that takes place on the polymer backbone might quench the electron transfer. However, if the polymer is expected to perform a catalytic reaction it needs to contain a moiety that can perform this chemical reaction.

Papers II and III focus on polymeric nanoparticles called Pdots based on the polymer PFBT as photocatalysts for fuel-forming reactions. A large pH effect was measured on the activity of the HER where it only was highly active in acidic conditions, which was attributed to the reaction of the BT-site

with acidic protons. It was shown in Paper III that this effect can be used to change the catalytic reaction to the reduction of CO_2 into CO by changing to basic conditions and changing the SD. For both of these reactions Pd, which has been proposed as the active catalytic site for the HER [76, 77], showed little to no impact on the catalytic activity. The chemical conditions are shown to be of key importance in these cases but currently, in the literature, they are often dictated by the SD. To move towards more practical catalytic systems the field should move away from SDs. Instead, we should look at full catalytic systems or use redox mediators where catalytic conditions can be optimised around the photocatalyst and to the catalytic reaction.

In Papers III and IV the reaction between reduced BT and CO_2 is studied. Interactions between BT and CO_2 are shown in both the PFBT polymer form and in the BTDN, where different reactions take place at three different reduction potentials. Pdots based on PFBT are shown to be selective photocatalysts, in basic conditions, for converting CO_2 into CO and the reaction seems to take place between two reduced BT units. BTDN is shown to bind CO_2 in all its three reduced states. It is also shown that one BTDN molecule can bind several CO_2 per unit likely up to four CO_2 molecules after being reduced twice. This binding is also proven to be mostly reversible upon oxidation. In its third reduction, BTDN can generate some CO and oxalate from a reduction process, albeit at what seems to be low efficiencies. The mechanism found for PFBT could inform the low efficiencies found in BTDN, that perhaps a closer proximity to other BT units could improve the reaction. Altering the reaction conditions of these catalysts would have a chance to improve them further, and the studies inform about how the catalysts could be modified to make them more active catalysts.

The research presented in this thesis has significantly advanced our understanding of fuel-forming reactions occurring on organic catalysts. Although the primary focus of this work has been on benzothiadiazole, the insights gained have broader implications for various systems. It is our hope that this research will serve as a catalyst for further mechanistic exploration of these catalytic reactions across different systems and inspire efforts to enhance their efficiency.

7. Popular Science Summary

Climate change is very much upon us, in the coming decades we will have to live with its repercussions. The time for action to do something about it has come and the most important step in altering these changes is a rapid swap to a sustainable, fossil-free, energy economy. The sun is by far the largest source of renewable energy that is available to us and of course, we need the sun to have life on earth. As solar energy from solar cells and other solar-driven forces like wind power is becoming cheaper and cheaper the biggest problem for an energy transition, from a technical standpoint, is not generating the energy but storing it. Storing electricity is not as easy as it might seem, even with the huge development of batteries in the last few decades the amount of electricity we would need to store is so large that batteries just don't become a practical solution.

A way of storing energy that we are very much used to handling in our infrastructure is chemical fuels, which are able to store a huge amount of energy while being more energy efficient than most other storage solutions. These renewable fuels such as for example hydrogen gas or methanol can be generated from basic easily accessible chemicals such as water or carbon dioxide but require an input of energy from light or electricity, but more importantly they require a catalyst for the reaction. A catalyst is a molecule or material that can make a chemical reaction go faster, without being used up in the reaction itself. Many chemical reactions are unlikely to take place at all without the use of a catalyst. To be able to develop and improve new catalysts for these purposes it is important to understand how the reactions work down on the chemical scale.

One type of catalyst that has piqued the interest of researchers in the last decade is light-active polymers. Polymers are long molecular chains with repeating molecular units with common examples such as plastic and cellulose. The type of light-active catalytic polymer is built out of two alternating building blocks one of which attracts electrons and the other pushes them away, giving it the name push-pull or donor-acceptor structure. This is the same type of material that can be found in an OLED TV where the polymers are activated by electricity to emit light. The opposite reaction can also take place where the polymers instead take up light and generate high-energy electrons, these electrons can then be used, either in a solar cell or to drive the generation of fuels. How these polymer catalysts work is still under investigation, which led to the work in this thesis. The building block in the polymer that is pulling

the electrons has been shown to be very important for the catalytic reaction. And, one of, if not the most important of these pulling building blocks is the molecular unit called benzothiadiazole or BT for short.

In this thesis, I have investigated the role that BT plays in the reaction when these renewable fuels are formed. I started by looking at the polymer PFBT it is quite a simple polymer built of a common "pushing" unit called fluorene and BT as the pulling unit. This polymer had already been shown to generate hydrogen gas from water and light, but how this worked was still a mystery. To investigate if BT could be the centre for this reaction the simple molecule BTDN was chosen as a good model for a part of the polymer. It was shown that BTDN indeed can act as a catalyst for the generation of hydrogen gas, with an in-depth description of how the reaction progresses on the microscopic scale. In the polymer itself, it turns out that the BT unit fills a similar role. Hydrogen gas is the simplest chemical one can imagine, built from two protons and two electrons. In the reaction where the hydrogen gas is generated the polymer will send two high-energy electrons but the protons will have to come from somewhere else. The protons should ideally come from water but they can also come from acidic protons in water, the acidic nature of something sour is simply reactive protons. It turns out that the polymer is much more active in generating hydrogen gas from acidic protons as compared to protons from water. This is because the reaction that takes place is similar to that of the molecule BTDN and requires the protons to be more reactive than those in water. The fact that this reaction was tunable by just altering the acidity of the water was utilised for the next project where instead of making hydrogen the aim was to make carbon dioxide react.

The project of removing carbon dioxide and making it back to something useful is huge for the transition into a sustainable society. Since BT was able to catalyse the reaction that makes hydrogen gas, we also investigated to see if it can bind up carbon dioxide and force it to react. Again the polymer PFBT was chosen to see if it could perform the reaction. If the reaction conditions were basic instead of acidic, so no reactive protons that can react to form hydrogen were present, it could be seen that the polymer can catalyse the reaction that makes carbon dioxide into carbon monoxide. While carbon monoxide is a toxic gas it is also valuable as a part of so-called synthesis gas or syngas that is useful for chemical synthesis in the chemical industry. The molecule BTDN was also investigated for the same reaction, BTDN can bind carbon dioxide which is valuable on its own, and it can also as a catalyst to generate small amounts of carbon monoxide and the ion oxalate.

So in conclusion, this thesis shows that benzothiadiazole a very common building block of light active polymers can act as a catalyst for many interesting fuel-forming reactions, something that was not known before this work.

8. Populärvetenskaplig Sammanfattning

Klimatet håller på att förändras, och under de kommande decennierna kommer vi att behöva leva med konsekvenserna av detta. Tiden för åtgärder har kommit, och det viktigaste steget för att bekämpa dessa förändringar är en snabb övergång till en hållbar, fossilfri energiekonomi. Solen är utan tvekan den största källan till förnybar energi som är tillgänglig för oss, och självklart behöver vi solen för att ha liv på jorden i vilket fall som helst. Eftersom solenergi från solceller och andra soldrivna energikällor så som vindkraft blir billigare och billigare, är det största problemet med en energiövergång, från en teknisk synpunkt, inte att generera energi, utan att lagra den. Att lagra elektricitet är inte så enkelt som det kan verka, även om batterier har kommit otroligt långt de senaste årtiondena är mängden elektricitet som vi skulle behöva lagra så stor att batterier helt enkelt inte är en praktisk lösning.

Ett sätt att lagra energi som vi är mycket vana vid att hantera är kemiska bränslen, och de kan lagra en enorm mängd energi samtidigt som de är tekniskt mindre komplicerade än de flesta andra möjlig lösningarna. Dessa förnybara bränslen, som till exempel vätegas eller metanol, kan genereras från grundläggande och lättillgängliga kemikalier som vatten eller koldioxid, men kräver en tillförsel av energi från ljus eller elektricitet, men ännu viktigare kräver de en katalysator för reaktionen. En katalysator är en molekyl eller material som kan påskynda en kemisk reaktion, utan att själv förbrukas i reaktionen. För många kemiska reaktioner är det osannolika att de kommer äga rum alls utan användning av en katalysator. För att kunna utveckla och förbättra nya katalysatorer för dessa ändamål är det viktigt att förstå hur reaktionerna fungerar på den kemiska skalan.

En typ av katalysator som har väckt forskarnas intresse de senaste tio åren är ljusaktiva polymerer. Polymerer är långa molekylära kedjor med upprepade molekylära enheter, exepmpel i vardagen är plaster och cellulosa. Den här typen av ljusaktiv katalytisk polymer är uppbyggd av två alternerande byggstenar, varav den ena attraherar elektroner och den andra skjuter bort dem, vilket ger den namnen push-pull eller donor-acceptor-struktur. Detta är samma typ av material som finns i en OLED-TV, där polymererna aktiveras av elektricitet för att avge ljus. Den motsatta reaktionen kan också äga rum, där polymererna istället tar upp ljus och genererar högenergi-elektroner. Dessa elektroner kan sedan användas antingen i en solcell eller för att driva produktionen av bränslen. Hur dessa polymerkatalysatorer fungerar är fortfarande inte känt,

vilket ledde till arbetet i denna avhandling. Byggstenen i polymeren som drar till sig elektronerna har visat sig vara mycket viktig för den katalytiska reaktionen, och en av de viktigaste av dessa byggstenar är molekylära enheten som kallas benzothiadiazol eller BT.

I den här avhandlingen har jag undersökt den roll som BT spelar i reaktionen när dessa förnybara bränslen bildas. Jag började med att titta på polymeren PFBT, som är ganska enkel och består av en vanlig "skjutande" enhet kallad fluoren och BT som den drar till elektroner. Den här polymeren hade redan visat sig kunna generera vätgas från vatten och ljus, men hur det fungerade var fortfarande en gåta. För att undersöka om BT kunde vara centrum för denna reaktion valdes den enkla molekylen BTDN som en bra modell för en del av polymeren. Det visade sig att BTDN kan fungera som en katalysator för generering av vätgas, och vi kunde beskriva reaktionen djupgåpå en mikroskopisk nivå. I själva polymeren visar det sig att BT-enheten fyller en liknande roll. Vätgas är den enklaste kemikalie man kan tänka sig, med två protoner och två elektroner. I reaktionen där vätgas genereras skickar polymeren ut två högenergetiska elektroner, men protonerna måste komma någon annanstans ifrån. Protonerna bör idealiskt komma från vatten, men de kan också komma från sura protoner i vatten, det som för något surt är helt enkelt reaktiva protoner. Det visar sig att polymeren är mycket mer aktiv i att generera vätegas från sura protoner jämfört med protoner från vatten. Det beror på att reaktionen som äger rum liknar den hos molekylen BTDN och kräver att protonerna är mer reaktiva än de som finns i vatten.

Att denna reaktion kunde styras genom att bara ändra vattens surhet användes för nästa projekt där syftet var att få koldioxid att reagera istället för att producera väte. Projektet att avlägsna koldioxid och göra den användbar är enormt viktigt för övergången till ett hållbart samhälle. Eftersom BT kunde katalysera reaktionen som producerar vätgas, undersökte vi också om den kunde binda koldioxid och tvinga den att reagera. Återigen valdes polymeren PFBT för att se om den kunde utföra reaktionen. Om reaktionsförhållandena var basiska istället för sura, så att inga reaktiva protoner som kan reagera för att bilda väte fanns närvarande, kunde det ses att polymeren kan katalysera reaktionen som omvandlar koldioxid till kolmonoxid. Kolmonoxid är en giftig gas så är den också värdefull som en del av så kallad syntesgas eller syngas som är användbar för kemisk syntes inom kemikalieindustrin. Molekylen BTDN undersöktes också för samma reaktion, och BTDN kan binda koldioxid, vilket är värdefullt i sig själv, och den kan också fungera som en katalysator för att generera små mängder kolmonoxid och jonen oxalat.

Sammanfattningsvis visar denna avhandling att benzothiadiazol, en mycket vanlig byggsten för ljusaktiva polymerer, kan fungera som katalysator för

många intressanta bränslebildande reaktioner, något som inte var känt innan detta arbete.

9. Acknowledgements

A PhD is a long and arduous process, and while it has been a fun challenge most of the time, I would not have been able to do it alone. I am immensely grateful for all of the people that has helped me with this accomplishment, in the lab, in discussions, with ideas, or just by being around when I needed to wind down.

Thank you **Haining Tian** for being a fantastic supervisor. Since, my first time in the group as a bachelor student I have always felt incredibly welcomed and supported with all of the projects we have tackled. I am grateful you always listened to my ideas but also that you kept me grounded when they became too high-flying.

My co-supervisor **Leif Hammarström**, thank you for always being a well of knowledge and inspiration. Your attitude and presence make this program a special place to do science.

A big thanks to all our external collaborators **Cleber Marchiori**, **Moyses Araujo**, **Ming Cheng**, **Ping Huang**, **Shaoqi Zhan**, **Ziyang Xia**, for all the invaluable work that ended up in this thesis. And an especially big thanks to **Michael Cheah** for all of the great insights and for being an inspiration in the lab.

Thanks to the Fyskem seniors **Erik Johansson**, **Erik Johansson**, **Gerrit Boschloo**, **Malin Johansson**, **Michal Maj**, **Reiner Lomoth**, **Starla Glover**, and **Victor Gray** for all the scientific input in courses and meetings.

Thank you **Alina Sekretareva**, **Ann Magnuson**, **Anna Arkhypchuk**, **Anders Thapper**, **Andreas Othaber**, **Eszter Borbas**, **Felix Ho**, **Gustav Berggren**, **Henrik Ottosson**, **Henrik Land**, **Karin Stensjö**, **Johannes Messinger**, **Nessima Salhi**, **Marcus Lundberg**, **Peter Lindblad**, **Pia Lindberg**, **Stefano Crespi** and **Sasha Ott** for always having something interesting to say and for generating the special research climate in Hus 7.

Thank you to all of the group members I have had the pleasure to work with during these years **Bo**, **David**, **Emil**, **Fangwen**, **Gaurav**, **Haoliang**, **Jing**, **Katerina**, **Naresh**, and **Sicong**. And a special thanks to **Aijie** and **Lei** for all the help getting me started when I was a newbie in the group!

Thank you, all of the office mates that have come and left **Alenka**, **Kelly**, **Lea**, **Ludo**, **Robin**, **Sara**, **Shihuai**, and all the present ones **Dylan**, **Minli**, and **Sree** for always making the office a welcoming space to be in. A special thanks to **Rima** for all the laughs and for being a great distraction when I should have really been focusing on this thesis.

Thank you, all of the **Fyskem** members I have not had the pleasure of sharing an office with **Andrew**, **Cathrine**, **Corentin**, **Hongwei**, **Min**, **Mohamed**, **Vitor**, and **Samir** it has always been a pleasure talking to you, science or otherwise.

And a big thanks to all of the non-physical chemists that have been around and making this stay way more enjoyable than it had any business being **Anna**, **Afridi Ashleigh**, **Casper**, **Claudia**, **Daniel**, **Holly**, **Jordann**, **Jorn**,**Josh**, **Kate**, **Max**, **Marco**, **Moritz**, **Nina**, **Nicholas**, **Nikos**, **Orkun**, **Paul**, **Salavat**, and **Sergii**.

A big thanks to the original **Wine Club**! **Robin**, **Vincent**, **Ben**, **Hemlata**, **João**, **Yocefu** and **Nidhi** for "inspiring" discussions and for making the first years in the lab such an awesome time. Thank you **Anđela**, **Giorgio**, and **Leigh Anna** for helping to keep the tradition going strong!

Big love to all of **SciPhi**! Thanks **Nora**, **Luca**, and **Beri** for being great friends and not only embracing my weird ideas and topics but even encouraging them!

Bin and **Carlos**. Thank you both for working so tirelessly on our projects in these final months! You are both wonderful colleagues, I am not sure I could have done it without you.

Sven. Thank you for always helping out with any lab issues, and for helping me shoulder the burden of the glove box and all the gases we need. You are the pillar of this department I don't know what they will do without you.

Mariia. You are an amazing coworker and friend, thank you for all the time we spent together in the lab and all the science we have discussed. Your joy always lightens the room the group would not be the same without you.

Brian. Thank you for being such a great friend and for being my mentor when I started and you are so humble you probably did not even think about it. Thank you for all of your hard work both in the lab and as a friend I look forward to seeing where your adventures lead us next!

Astrid and **Belinda**. Thank you for always being there in the office when I needed to go or talk some nonsense. I am so happy to have shared an office with both of you I could not have asked for better role models and friends during my time here!

Sigrid. Thank you for sharing this journey all the way with me, we have gone through the thick of it together and I am happy it was you who I shared the journey with. Thank you for being such a good friend and supporter through it all, soon it will be your turn and I plan to be cheering you on all the way!

Sina. Thank you for always being up for scientific discussions or solving issues in the lab and even more for being a great friend.
Andrea I am so grateful to have you as a friend that I can talk about literally everything, from the wave function of the universe to personal problems. You are the heart of fyskem going forward and it is in great hands. Thank you both for helping me correct this thesis, I hope it turned out legible in the end!

Till familjen, **Mamma**, **Pappa**, **Malin**, och **Kerstin** för allt erat omåttliga stöd!

Och till sist men sannerligen inte minst **Uppsala Gänget**, **Benjamin**, **Dennis**, **Isabel**, **Linn**, **Linn**, and **Robin**. Tack för att ni är de bästa vännerna tänkbara och för all support genom alla dessa år. Doktorandtiden hade inte varit den samma utan er!

Finally thanks to everyone whom I failed to mention, there are more people to thank than what I can fit in this book or what I can remember!

Bibliography

(1) Rockström, J.; Steffen, W.; Noone, K.; Persson, III, F. S. C.; Lambin, E. F.; Lenton, T. M.; Scheffer, M.; Folke, C.; Schellnhuber, H. J.; Nykvist, B.; de Wit, C. A.; Hughes, T.; van der Leeuw, S.; Rodhe, H.; Sörlin, S.; Snyder, P. K.; Costanza, R.; Svedin, U.; Falkenmark, M.; Karlberg, L.; Corell, R. W.; Fabry, V. J.; Hansen, J.; Walker, B.; Liverman, D.; Richardson, K.; Crutzen, P.; Foley, J. A. A safe operating space for humanity. *Nature* **2009**, *461*, 472–475.

(2) Steffen, W.; Richardson, K.; Rockström, J.; Cornell, S. E.; Fetzer, I.; Bennett, E. M.; Biggs, R.; Carpenter, S. R.; de Vries, W.; de Wit, C. A.; Folke, C.; Gerten, D.; Heinke, J.; Mace, G. M.; Persson, L. M.; Ramanathan, V.; Reyers, B.; Sörlin, S. Planetary boundaries: Guiding human development on a changing planet. *Science* **2015**, *347*, 1259855.

(3) Waters, C. N.; Zalasiewicz, J.; Summerhayes, C.; Barnosky, A. D.; Poirier, C.; Galuszka, A.; Cearreta, A.; Edgeworth, M.; Ellis, E. C.; Ellis, M.; Jeandel, C.; Leinfelder, R.; McNeill, J. R.; deB. Richter, D.; Steffen, W.; Syvitski, J.; Vidas, D.; Wagreich, M.; Williams, M.; Zhisheng, A.; Grinevald, J.; Odada, E.; Oreskes, N.; Wolfe, A. P. The Anthropocene is functionally and stratigraphically distinct from the Holocene. *Science* **2016**, *351*, aad2622.

(4) Arrhenius, S. On the Influence of Carbonic Acid in the Air upon the Temperature of the Ground. *Philosophical Magazine and Journal of Science* **1896**, *41*, 237–276.

(5) Pörtner, H.-O.; Roberts, D.; Tignor, M.; Poloczanska, E.; Mintenbeck, K.; Alegría, A.; Craig, M.; Langsdorf, S.; Löschke, S.; Möller, V.; Okem, A.; (eds.), B. R., *Climate Change 2022: Impacts, Adaptation, and Vulnerability. Contribution of Working Group II to the Sixth Assessment Report of the Intergovernmental Panel on Climate Change*; IPCC Report; Cambridge University Press: 2022.

(6) Perez, R.; Perez, M. A Fundamental Look At Supply Side Energy Reserves For The Planet. *SHC/IEA Solar Update* **2015**, *62*, 4–5.

(7) Suri, M.; Betak, J.; Rosina, K.; Chrkavy, D.; Suriova, N.; Cebecauer, T.; Caltik, M.; Erdelyi, B. *Global Photovoltaic Power Potential by Country*; 2020.

(8) Winter, M.; Brodd, R. J. What Are Batteries, Fuel Cells, and Supercapacitors? *Chemical Reviews* **2004**, *104*, 4245–4270.

(9) Nelson, N.; Ben-Shem, A. The complex architecture of oxygenic photosynthesis. *Nature Reviews Molecular Cell Biology* **2004**, *5*, 971–982.

(10) Eberhard, S.; Finazzi, G.; André, W. F. The dynamics of photosynthesis. *Annual Review of Genetics* **2008**, *42*, 463–515.

(11) Dogutan, D. K.; Nocera, D. G. Artificial Photosynthesis at Efficiencies Greatly Exceeding That of Natural Photosynthesis. *Accounts of Chemical Research* **2019**, 3143–3148.

(12) Tachibana, Y.; Vayssieres, L.; Durrant, J. R. Artificial photosynthesis for solar water-splitting. *Nature Photonics* **2012**, *6*, 511–518, DOI: 10.1038/nphoton.2012.175.

(13) Bushuyev, O. S.; De Luna, P.; Dinh, C. T.; Tao, L.; Saur, G.; van de Lagemaat, J.; Kelley, S. O.; Sargent, E. H. What Should We Make with CO2 and How Can We Make It? *Joule* **2018**, *2*, 825–832, DOI: 10.1016/j.joule.2017.09.003.

(14) Kondepudi, D.; Prigogine, I., *Modern Thermodynamics*; John Wiley & Sons: 1999.

(15) Arrhenius, S. Über die Dissociationswärme und den Einfluss der Temperatur auf den Dissociationsgrad der Elektrolyte. *Zeitschrift für Physikalische Chemie* **1889**, *4U*, 96–116, DOI: doi:10.1515/zpch-1889-0408.

(16) Espenson, J. H., *Chemical Kinetics and Reaction Mechanisms*; McGraw-Hill Book Company: 1981.

(17) Zhang, L.; Mohamed, H. H.; Dillert, R.; Bahnemann, D. Kinetics and mechanisms of charge transfer processes in photocatalytic systems: A review. *Journal of Photochemistry and Photobiology C: Photochemistry Reviews* **2012**, *13*, 263–276, DOI: 10.1016/J.JPHOTOCHEMREV.2012.07.002.

(18) Wodrich, M. D.; Sawatlon, B.; Busch, M.; Corminboeuf, C. The Genesis of Molecular Volcano Plots This is an initial proof-of-principle. *Acc. Chem. Res* **2015**, *6*, 2023, DOI: 10.1021/acs.accounts.0c00857.

(19) Dubois, M. R.; Dubois, D. L. The roles of the first and second coordination spheres in the design of molecular catalysts for H 2 production and oxidationw. *Chem. Soc. Rev.*, *38*, 62–72, DOI: 10.1039/b801197b.

(20) Stripp, S. T.; Duffus, B. R.; Fourmond, V.; Léger, C.; Leimkü, S.; Hirota, S.; Hu, Y.; Jasniewski, A.; Ogata, H.; Ribbe, M. W. Second and Outer Coordination Sphere Effects in Nitrogenase, Hydrogenase, Formate Dehydrogenase, and CO Dehydrogenase. **2022**, DOI: 10.1021/acs.chemrev.1c00914.

(21) Bhunia, S.; Ghatak, A.; Dey, A. Second Sphere Effects on Oxygen Reduction and Peroxide Activation by Mononuclear Iron Porphyrins and Related Systems. *Chemical Reviews* **2022**, *122*, 12370–12426, DOI: 10.1021/acs.chemrev.1c01021.

(22) Wiedner, E. S.; Appel, A. M.; Raugei, S.; Shaw, W. J.; Bullock, R. M. Molecular Catalysts with Diphosphine Ligands Containing Pendant Amines. *Chemical Reviews* **2022**, *122*, 12427–12474, DOI: 10.1021/acs.chemrev.1c01001.

(23) Zhang, B.; Sun, L. Why nature chose the Mn 4 CaO 5 cluster as water-splitting catalyst in photosystem II: a new hypothesis for the mechanism of O-O bond formation. *Dalton Transaction* **2018**, *47*, 14381, DOI: 10.1039/c8dt01931b.

(24) Simmons, T. R.; Berggren, G.; Bacchi, M.; Fontecave, M.; Artero, V. Mimicking hydrogenases: From biomimetics to artificial enzymes, 2014, DOI: 10.1016/j.ccr.2013.12.018.

(25) Wittkamp, F.; Senger, M.; Stripp, S. T.; Apfel, U.-P. ChemComm Chemical Communications [FeFe]-Hydrogenases: recent developments and future perspectives. *Chem. Commun* **2018**, *54*, 5934, DOI: 10.1039/c8cc01275j.

(26) Chen, C.; Li, Y.; Zhao, G.; Yao, R.; Zhang, C. Natural and Artificial Mn 4 Ca Cluster for the Water Splitting Reaction. *ChemSusChem* **2017**, *10*, 4403–4408, DOI: 10.1002/cssc.v10.22.

(27) White, J. L.; Baruch, M. F.; Pander, J. E.; Hu, Y.; Fortmeyer, I. C.; Park, J. E.; Zhang, T.; Liao, K.; Gu, J.; Yan, Y.; Shaw, T. W.; Abelev, E.; Bocarsly, A. B. Light-Driven Heterogeneous Reduction of Carbon Dioxide: Photocatalysts and Photoelectrodes. **2015**, DOI: 10.1021/acs.chemrev.5b00370.

(28) Saha, P.; Amanullah, S.; Dey, A. Selectivity in Electrochemical CO_2 Reduction. *J. Am. Chem. Soc* **2022**, *137*, 18, DOI: 10.1021/acs.accounts.1c00678.

(29) Curtis, C. J.; Miedaner, A.; Ciancanelli, R.; Ellis, W. W.; Noll, B. C.; DuBois, M. R.; DuBois, D. L. [Ni(Et2PCH2NMeCH2PEt2)2]2+ as a Functional Model for Hydrogenases. *Inorganic Chemistry* **2002**, *42*, 216–227, DOI: 10.1021/ic020610v.

(30) Wilson, A. D.; Newell, R. H.; McNevin, M. J.; Muckerman, J. T.; DuBois, M. R.; DuBois, D. L. Hydrogen Oxidation and Production Using Nickel-Based Molecular Catalysts with Positioned Proton Relays. *Journal of the American Chemical Society* **2005**, *128*, 358–366, DOI: 10.1021/ja056442y.

(31) Collman, J. P.; Brauman, J. I.; Doxsee, K. M.; Halbert, T. R.; Suslick, K. S. Model compounds for the T state of hemoglobin (cobalt-substituted hemoproteins/cooperativity/hemoproteins/myoglobin/oxygen binding). **1978**, *75*, 564–568.

(32) Grodkowski, J.; Behar, D.; Neta, P.; Hambright, P. Iron Porphyrin-Catalyzed Reduction of CO 2. Photochemical and Radiation Chemical Studies. *Proc. Nati. Acad. Sci.* **1997**, *75*, 564–568.

(33) Anxolabéhére-Mallart, E.; Bonin, J.; Fave, C.; Robert, M. Small-molecule activation with iron porphyrins using electrons, photons and protons: some recent advances and future strategies. *Dalton Trans* **2019**, *48*, 5869, DOI: 10.1039/c9dt00136k.

(34) Montoya, J. H.; Seitz, L. C.; Chakthranont, P.; Vojvodic, A.; Jaramillo, T. F.; NOrskov, J. K. Materials for solar fuels and chemicals. *Nature Materials* **2016**, *16*, DOI: 10.1038/NMAT4778.

(35) Sun, L.; Reddu, V.; Fisher, A. C.; Wang, X. Electrocatalytic reduction of carbon dioxide: opportunities with heterogeneous molecular catalysts. *Energy Environ. Sci.* **2020**, *13*, 374–403, DOI: 10.1039/C9EE03660A.

(36) She, Z. W.; Kibsgaard, J.; Dickens, C. F.; Chorkendorff, I.; NÃ¸rskov, J. K.; Jaramillo, T. F. Combining theory and experiment in electrocatalysis: Insights into materials design. *Science* **2017**, *355*, DOI: 10.1126/science.aad4998.

(37) Liu, M.; Zhao, Z.; Duan, X.; Huang, Y.; Liu, M.; Duan, X.; Zhao, Z.; Huang, Y. Nanoscale Structure Design for High-Performance Pt-Based ORR Catalysts. **2018**, DOI: 10.1002/adma.201802234.

(38) Su, Z.; Chen, T.; Su, Z.; Chen, T. Porous Noble Metal Electrocatalysts: Synthesis, Performance, and Development. *Small* **2021**, 2005354, DOI: 10.1002/smll.202005354.

(39) Wang, Z.; Tang, M. T.; Cao, A.; Chan, K.; Norskov, J. K. Insights into the Hydrogen Evolution Reaction on 2D Transition-Metal Dichalcogenides. *Journal of Physical Chemistry C* **2022**, *126*, 5151–5158, DOI: 10.1021/ACS.JPCC.1C10436/SUPPL_FILE/JP1C10436_SI_001.PDF.

(40) Bagger, A.; Ju, W.; Varela, A. S.; Strasser, P.; Rossmeisl, J. Electrochemical CO2 Reduction: Classifying Cu Facets. *ACS Catalysis* **2019**, *9*, 7894–7899, DOI: 10.1021/acscatal.9b01899.

(41) Kim, Y.-G.; Baricuatro, J. H.; Javier, A.; Gregoire, J. M.; Soriaga, M. P. The Evolution of the Polycrystalline Copper Surface, First to Cu(111) and Then to Cu(100), at a Fixed CO2RR Potential: A Study by Operando EC-STM. *Langmuir* **2014**, *30*, 15053–15056, DOI: 10.1021/la504445g.

(42) Correlating Oxidation State and Surface Area to Activity from Operando Studies of Copper CO Electroreduction Catalysts in a Gas-Fed Device. *ACS Catalysis* **2020**, *10*, 8000–8011, DOI: 10.1021/acscatal.0c01670.

(43) Ren, S.; Joulié, D.; Salvatore, D.; Torbensen, K.; Wang, M.; Robert, M.; Berlinguette, C. P. Molecular electrocatalysts can mediate fast, selective CO2 reduction in a flow cell. *Science* **2019**, *365*, 367–369, DOI: 10.1126/science.aax4608.

(44) Whang, D. R. Immobilization of molecular catalysts for artificial photosynthesis. **2020**, *7*, 37, DOI: 10.1186/s40580-020-00248-1.

(45) Jiao, L.; Wang, Y.; Jiang, H.-L.; Xu, Q. Metal-Organic Frameworks as Platforms for Catalytic Applications. **2017**, DOI: 10.1002/adma.201703663.

(46) Suremann, N. F.; Mccarthy, B. D.; Gschwind, W.; Kumar, A.; Johnson, B. A.; Hammarström, L.; Ott, S. Molecular Catalysis of Energy Relevance in Metal-Organic Frameworks: From Higher Coordination Sphere to System Effects. **2023**, DOI: 10.1021/acs.chemrev.2c00587.

(47) Bhattacharyya, D.; Videla, P. E.; Cattaneo, M.; Batista, V. S.; Lian, T.; Kubiak, C. P. Vibrational Stark shift spectroscopy of catalysts under the influence of electric fields at electrode-solution interfaces. *Chem. Sci* **2021**, *12*, 10131–10149, DOI: 10.1039/d1sc01876k.

(48) Kaminsky, C. J.; Weng, S.; Wright, J.; Surendranath, Y. Adsorbed cobalt porphyrins act like metal surfaces in electrocatalysis. *Nature Catalysis* **2022**, *5*, 430–442, DOI: 10.1038/s41929-022-00791-6.

(49) Johnson, B. A.; Beiler, A. M.; McCarthy, B. D.; Ott, S. Transport Phenomena: Challenges and Opportunities for Molecular Catalysis in Metal-Organic Frameworks. *J. Am. Chem. Soc* **2020**, *142*, 11941–11956, DOI: 10.1021/jacs.0c02899.

(50) Liu, J.; Wang, H.; Antonietti, M. Graphitic carbon nitride "reloaded": emerging applications beyond (photo)catalysis. *2308 | Chem. Soc. Rev* **2016**, *45*, 2308, DOI: 10.1039/c5cs00767d.

(51) Tang, C.; Cheng, M.; Lai, C.; Li, L.; Yang, X.; Du, L.; Zhang, G.; Wang, G.; Yang, L. Recent progress in the applications of non-metal modified graphitic carbon nitride in photocatalysis. *Coordination Chemistry Reviews* **2023**, *474*, 214846, DOI: 10.1016/J.CCR.2022.214846.

(52) Hu, X.-L.; Li, H.-G.; Tan, B.-E. COFs-based Porous Materials for Photocatalytic Applications. *Chinese J. Polym. Sci.* **2020**, *38*, 673â684, DOI: 10.1007/s10118-020-2394-x.

(53) Yang, Q.; Luo, M.; Liu, K.; Cao, H.; Yan, H. Covalent organic frameworks for photocatalytic applications. *Applied Catalysis B: Environmental* **2020**, *276*, 119174, DOI: 10.1016/J.APCATB.2020.119174.

(54) Wang, Y.; Vogel, A.; Sachs, M.; Sprick, R. S.; Wilbraham, L.; Moniz, S. J.; Godin, R.; Zwijnenburg, M. A.; Durrant, J. R.; Cooper, A. I.; Tang, J. Current understanding and challenges of solar-driven hydrogen generation using polymeric photocatalysts. *Nature Energy* **2019**, *4*, 746–760, DOI: 10.1038/s41560-019-0456-5.

(55) Pavliuk, M. V.; Wrede, S.; Liu, A.; Brnovic, A.; Wang, S.; Axelsson, M.; Tian, H. Preparation, characterization, evaluation and mechanistic study of organic polymer nano-photocatalysts for solar fuel production. *Chemical Society Reviews* **2022**, *51*, 6909–6935, DOI: 10.1039/d2cs00356b.

(56) Yanagida, S.; Kabumoto, A.; Mizumoto, K.; Pac, C.; Yoshino, K. Poly (p-phenylene) Catalysed Photoreduction of Water to Hydrogen. *J. Chem. Soc., Chem. Commun.* **1985**, 474–475.

(57) Matsuoka., S.; Fujii, H.; Yamada, T.; Pac, C.; Ishida, A.; Takamuku, S.; Kusaba, M.; Nakashima, N.; Yanagida, S. Photocatalysis of Oligo(p-phenylenes). Photoreductlve Production of Hydrogen and Ethanol In Aqueous Triethylamine. *J. Phys. Chem.* **1991**, *95*, 5802–5808.

(58) Wang, X.; Maeda, K.; Thomas, A.; Takanabe, K.; Xin, G.; Carlsson, J. M.; Domen, K.; Antonietti, M. A metal-free polymeric photocatalyst for hydrogen production from water under visible light. *Nature Materials* **2009**, *8*, 76–80, DOI: 10.1038/nmat2317.

(59) Sprick, R. S.; Jiang, J.; Bonillo, B.; Ren, S.; Ratvijitvech, T.; Guiglion, P.; Zwijnenburg, M.; Adams, D.; Cooper, A. Tunable organic photocatalysts for visible-light-driven hydrogen evolution. *J. Am. Chem. Soc* **2015**, *137*, 3265–3270, DOI: 10.1021/ja511552k.

(60) Wang, L.; Fernández-Terán, R.; Zhang, L.; Fernandes, D. L. A.; Tian, L.; Chen, H.; Tian, H. Organic Polymer Dots as Photocatalysts for Visible Light-Driven Hydrogen Generation. *Angew. Chem. Int. Ed* **2016**, *128*, 12494–12498, DOI: 10.1002/ange.201607018.

(61) Sachs, M.; Sprick, R. S.; Pearce, D.; Hillman, S. A.; Monti, A.; Guilbert, A. A.; Brownbill, N. J.; Dimitrov, S.; Shi, X.; Blanc, F.; Zwijnenburg, M. A.; Nelson, J.; Durrant, J. R.; Cooper, A. I. Understanding structure-activity relationships in linear polymer photocatalysts for hydrogen evolution. *Nature Communications* **2018**, *9*, DOI: 10.1038/s41467-018-07420-6.

(62) Liu, A.; Gedda, L.; Axelsson, M.; Pavliuk, M.; Edwards, K.; Hammarström, L.; Tian, H. Panchromatic ternary polymer dots involving sub-picosecond energy and charge transfer for efficient and stable photocatalytic hydrogen evolution. *J. Am. Chem. Soc* **2021**, *143*, DOI: 10.1021/jacs.0c12654.

(63) Havinga, E.; Hoeve, W. t.; Wynberg, H. A new class of small band gap organic polymer conductors. *Polymer Bulletin* **1992**, *29*, 119–126.

(64) Havinga, E.; Hoeve, W. t.; Wynberg, H. Alternate donor-acceptor small-band-gap semiconducting polymers; Polysquaraines and polycroconaines. *Synthetic Metals* **1993**, *55*, 299–306.

(65) Shao, S.; Wang, L. Through-space charge transfer polymers for solution-processed organic light-emitting diodes. *Aggregate* **2020**, *1*, 45â56, DOI: 10.1002/agt2.4.

(66) Günes, S.; Neugebauer, H.; Sariciftci, N. S. Conjugated Polymer-Based Organic Solar Cells. *Chemical Reviews* **2007**, *107*, 1324–1338, DOI: 10.1021/cr050149z.

(67) Holliday, S.; Li, Y.; Luscombe, C. K. Recent advances in high performance donor-acceptor polymers for organic photovoltaics. *Progress in Polymer Science* **2017**, *70*, 34–51, DOI: 10.1016/J.PROGPOLYMSCI.2017.03.003.

(68) Pellegrin, Y.; Odobel, F. Sacrificial electron donor reagents for solar fuel production. *Comptes Rendus Chimie* **2017**, *20*, 283–295, DOI: 10.1016/j.crci.2015.11.026.

(69) Stegbauer, L.; Schwinghammer, K.; Lotsch, B. V. A hydrazone-based covalent organic framework for photocatalytic hydrogen production. *Chem. Sci* **2014**, *85*, 2789–2793, DOI: 10.1039/c4sc00016a.

(70) Sprick, R. S.; Bonillo, B.; Clowes, R.; Guiglion, P.; Slater, B. J.; Blanc, F.; Zwijnenburg, M. A.; Adams, D. J.; Cooper, A. I. Photocatalysis Hot Paper Visible-Light-Driven HydrogenEvolution UsingPlanarized Conjugated Polymer Photocatalysts. *Angew. Chem. Int. Ed*, *55*, 1792–1796, DOI: 10.1002/ange.201510542.

(71) Demchenko, A. P. Methods and Applications in Fluorescence Photobleaching of organic fluorophores: quantitative characterization, mechanisms, protection. *Methods Appl. Fluoresc* **2020**, *8*, 022001, DOI: 10.1088/2050-6120/ab7365.

(72) Gupta, R.; Darwish, G. H.; Algar, W. R. Complex Photobleaching Behavior of Semiconducting Polymer Dots. *J. Phys. Chem. C* **2022**, *126*, 20960–20974, DOI: 10.1021/acs.jpcc.2c07039.

(73) Hillman, S. A. J.; Sprick, R. S.; Pearce, D.; Woods, D. J.; Sit, W.-Y.; Shi, X.; Cooper, A. I.; Durrant, J. R.; Nelson, J. Why Do Sulfone-Containing Polymer Photocatalysts Work So Well for Sacrificial Hydrogen Evolution from Water? *J. Am. Chem. Soc.* **2022**, *144*, 19382–19395.

(74) Miyaura, N.; Yamada, K.; Suzuki, A. A new Stereospecific Cross-Coupling by the Palladium-Catalyzed Reaction of 1-Alkeneboranes with 1-Alkenyl or I-Alkynyl Halides. *Tetrahedron Letters* **1979**, 3437–3440.

(75) Miyaura, N.; Suzuki, A. Palladium-Catalyzed Cross-Coupling Reactions of Organoboron Compounds. *Chemical Reviews* **1995**, *95*, 2457–2483, DOI: 10.1021/cr00039a007.

(76) Kosco, J.; Sachs, M.; Godin, R.; Kirkus, M.; Francas, L.; Bidwell, M.; Qureshi, M.; Anjum, D.; Durrant, J. R.; McCulloch, I. The Effect of Residual Palladium Catalyst Contamination on the Photocatalytic Hydrogen Evolution Activity of Conjugated Polymers. *Advanced Energy Materials* **2018**, *8*, DOI: 10.1002/aenm.201802181.

(77) Sachs, M.; Cha, H.; Kosco, J.; Aitchison, C. M.; s, L. F.; Corby, S.; Chiang, C.-L.; Wilson, A. A.; Godin, R.; Fahey-Williams, A.; Cooper, A. I.; Sprick, R. S.; McCulloch, I.; Durrant, J. R. Tracking Charge Transfer to Residual Metal Clusters in Conjugated Polymers for Photocatalytic Hydrogen Evolution. *J. Am. Chem. Soc.* **2020**, *142*, 14574–14587, DOI: 10.1021/jacs.0c06104.

(78) Pati, P. B.; Damas, G.; Tian, L.; Fernandes, D. L. A.; Zhang, L.; Pehlivan, I. B.; Edvinsson, T.; Araujo, C. M.; Tian, H. An experimental and theoretical study of an efficient polymer nano-photocatalyst for hydrogen evolution. *Energy and Environmental Science* **2017**, *10*, 1372–1376, DOI: 10.1039/c7ee00751e.

(79) Bai, Y.; Wilbraham, L.; Slater, B. J.; Zwijnenburg, M. A.; Sprick, R. S.; Cooper, A. I. Accelerated Discovery of Organic Polymer Photocatalysts for Hydrogen Evolution from Water through the Integration of Experiment and Theory. *Journal of the American Chemical Society* **2019**, *141*, 9063–9071, DOI: 10.1021/jacs.9b03591.

(80) Menke, S. M.; Holmes, R. J. Excition diffusion in organic photovoltaic cells. *Energy Environ. Sci* **2014**, *7*, 499–512, DOI: 10.1039/c3ee42444h.

(81) Mikhnenko, O. V.; Blom, P. W. M.; Nguyen, T.-Q. Exciton diffusion in organic semiconductors. *Energy Environ. Sci* **2015**, *8*, 1867, DOI: 10.1039/c5ee00925a.

(82) Wadsworth, A.; Hamid, Z.; Kosco, J.; Gasparini, N.; Mcculloch, I. The Bulk Heterojunction in Organic Photovoltaic, Photodetector, and Photocatalytic Applications. *Adv. Mater.* **2020**, *32*, 2001763, DOI: 10.1002/adma.202001763.

(83) Kosco, J.; Bidwell, M.; Cha, H.; Martin, T.; Howells, C. T.; Sachs, M.; Anjum, D. H.; Lopez, S. G.; Zou, L.; Wadsworth, A.; Zhang, W.; Zhang, L.; Tellam, J.; Sougrat, R.; Laquai, F.; DeLongchamp, D. M.; Durrant, J. R.; McCulloch, I. Enhanced photocatalytic hydrogen evolution from organic semiconductor heterojunction nanoparticles. *Nature Materials*, *19*, 559–565, DOI: 10.1038/s41563-019-0591-1.

(84) Kosco, J.; Gonzalez-Carrero, S.; Howells, C. T.; Fei, T.; Dong, Y.; Sougrat, R.; Harrison, G. T.; Firdaus, Y.; Sheelamanthula, R.; Purushothaman, B.; Moruzzi, F.; Xu, W.; Zhao, L.; Basu, A.; De Wolf, S.; Anthopoulos, T. D.; Durrant, J. R.; McCulloch, I. Generation of long-lived charges in organic semiconductor heterojunction nanoparticles for efficient photocatalytic hydrogen evolution. *Nature Energy* **2022**, *7*, 340–351, DOI: 10.1038/s41560-022-00990-2.

(85) Mullekom, H. A. M. V.; Vekemans, J. A. J. M.; Meijer, E. W. Alternating copolymer of pyrrole and 2,1,3-benzothiadiazole. *Chem. Commun* **1996**, *9*, 2163–2164, DOI: 10.1039/CC9960002163.

(86) Wang, Y.; Michinobu, T. Benzothiadiazole and its *mathrm*π-extended, heteroannulated derivatives: Useful acceptor building blocks for high-performance donor-acceptor polymers in organic electronics. *J. Mater. Chem. C* **2016**, *4*, 6200–6214, DOI: 10.1039/c6tc01860b.

(87) Nie, Q.; Tang, A.; Guo, Q.; Zhou, E. Benzothiadiazole-based non-fullerene acceptors. *Nano Energy* **2021**, *87*, 106174, DOI: 10.1016/J.NANOEN.2021.106174.

(88) Parker, T. C.; Patel, D. G.; Moudgil, K.; Barlow, S.; Risko, C.; Brédas, J.-L.; Reynolds, J. R.; Marder, S. R. Heteroannulated acceptors based on benzothiadiazole. *Mater. Horiz* **2015**, *2*, 22–36, DOI: 10.1039/c4mh00102h.

(89) Yang, X.; Walpita, J.; Mirzakulova, E.; Oottikkal, S.; Hadad, C. M.; Glusac, K. D. Mechanistic Studies of Electrode-Assisted Catalytic Oxidation by Flavinium and Acridinium Cations. **2014**, *4*, 2635â2644, DOI: 10.1021/cs5005135.

(90) Li, H.; Xie, F.; Zhang, M.-T. Metal-Free Electrocatalyst for Water Oxidation Initiated by Hydrogen Atom Transfer. **2023**, *11*, 46, DOI: 10.1021/acscatal.0c04606.

(91) Dolganov, A. V.; Tanaseichuk, B. S.; Moiseeva, D. N.; Yurova, V. Y.; Sakanyan, J. R.; Shmelkova, N. S.; Lobanov, V. V. Acridinium salts as metal-free electrocatalyst for hydrogen evolution reaction. *Electrochemistry Communications* **2016**, *68*, 59–61, DOI: 10.1016/J.ELECOM.2016.04.015.

(92) Dolganov, A. V.; Tanaseichuk, B. S.; Yurova, V. Y.; Chernyaeva, O. Y.; Okina, E. V.; Balandina, A. V.; Portnova, E. A.; Kozlov, A. S.; Solovyova, E. O.; Yudina, A. D.; Akhmatova, A. A.; Lyukshina, Y. I. Moving from acridinium to pyridinium: From complex to simple. 2,4,6-Triphenylpyridine and 2,4,6-triphenylpyrilium perchlorate as "metal-free" electrocatalysts of hydrogen evolution reaction (HER): The influence of the nature of the heteroatom and acid on the pathway HER. *International Journal of Hydrogen Energy* **2019**, *44*, 21495–21505, DOI: 10.1016/J.IJHYDENE.2019.06.067.

(93) Axelsson, M.; Marchiori, C.; Huang, P.; Araujo, C.; Tian, H. Small Organic Molecule Based on Benzothiadiazole for Electrocatalytic Hydrogen Production. *J. Am. Chem. Soc* **2021**, *143*, DOI: 10.1021/jacs.1c10600.

(94) Karak, P.; Mandal, S. K.; Choudhury, J. Exploiting the NADP+/NADPH-like Hydride-Transfer Redox Cycle with Bis-Imidazolium-Embedded Heterohelicene for Electrocatalytic Hydrogen Evolution Reaction. *J. Am. Chem. Soc* **2023**, *0*, DOI: 10.1021/jacs.3c04737.

(95) Ilic, S.; Kadel, U. P.; Basdogan, Y.; Keith, J. A.; Glusac, K. D. Thermodynamic Hydricities of Biomimetic Organic Hydride Donors. *J. Am. Chem. Soc* **2018**, *140*, 11, DOI: 10.1021/jacs.7b13526.

(96) Ilic, S.; Gesiorski, J. L.; Weerasooriya, R. B.; Glusac, K. D. Biomimetic Metal-Free Hydride Donor Catalysts for CO 2 Reduction. *J. Phys. Chem. Lett.* **2021**, *140*, 4569â4579, DOI: 10.1021/acs.accounts.1c00708.

(97) Karak, P.; Mandal, K.; Choudhury, J. Bis-Imidazolium-Embedded Heterohelicene: A Regenerable NADP + Cofactor Analogue for Electrocatalytic CO 2 Reduction. *J. Am. Chem. Soc* **2023**, *145*, 16, DOI: 10.1021/jacs.2c12883.

(98) Ceballos, B. M.; Yang, J. Y. Directing the reactivity of metal hydrides for selective CO2 reduction. *Proceedings of the National Academy of Sciences of the United States of America* **2018**, *115*, 12686–12691, DOI: 10.1073/pnas.1811396115.

(99) Gagliardi, C. J.; Vannucci, A. K.; Concepcion, J. J.; Chen, Z.; Meyer, T. J. The role of proton coupled electron transfer in water oxidation Broader context. **2012**, *5*, 7704–7717, DOI: 10.1039/c2ee03311a.

(100) Nam, D.-H.; Luna, P. D.; Rosas-Hernández, A.; Thevenon, A.; Li, F.; Agapie, T.; Peters, J. C.; Shekhah, O.; Eddaoudi, M.; Sargent, E. H. Molecular enhancement of heterogeneous CO2 reduction. *Nature Materials* **2020**, *19*, 266–276, DOI: 10.1038/s41563-020-0610-2.

(101) Creissen, C. E.; Cruz, G. R. D. L.; Karapinar, D.; Taverna, D.; Schreiber, M. W.; Fontecave, M. Molecular Inhibition for Selective CO2 Conversion. *Angew. Chem. Int. Ed.* **2022**, *61*, e202206279, DOI: 10.1002/anie.202206279.

(102) Schrödinger, E. An Undulatory Theory of the Mechanics of Atoms and Molecules. *Physical Review* **1926**, *28*, 1049–1070.

(103) Heisenberg, W. Uber quantentheoretische Umdeutung kinematischer und mechaniseher Beziehungen. *Physik* **1925**, *33*, 879–893.

(104) Feynman, R. Space-Time Approach to Non-Relativistic Quantum Mechanics. *Reviews of Modern Physics* **1948**, *20*, 367–387.

(105) Wright, D.; Sangtarash, S.; Mueller, N. S.; Lin, Q.; Sadeghi, H.; Baumberg, J. J. Vibrational Stark Effects: Ionic Influence on Local Fields. *The Journal of Physical Chemistry Letters* **2022**, *13*, 4905–4911, DOI: 10.1021/acs.jpclett.2c01048.

(106) Atkins, P.; de Paula, J., *Atkins' Physical Chemistry*, 8th; W. H. Freeman and Company: 2006.

(107) Atkins, P.; Friedman, R., *Molecular Quantum Mechanics*, 4th; Oxford University Press: 2005.

(108) Bard, A. J.; Faulkner, L. R., *Electrochemical methods: fundamentals and applications*, 2nd, 2001; Vol. 2nd.

(109) Savéant, J.-M., *Elements of Molecular and Biomolecular Electrochemistry An Electrochemical Approach to Electron Transfer Chemistry*, 2006.

(110) Fick, A. V. On liquid diffusion. *The London, Edinburgh, and Dublin Philosophical Magazine and Journal of Science* **1855**, *10*, 30–39, DOI: 10.1080/14786445508641925.

(111) Faraday, M. Experimental Researches in Electricity.-Fifth Series. *Philos. Trans. R. Soc. London* **1833**, *123*, 675–710.

(112) Faraday, M. Experimental Researches in Electricity. Seventh Series. *Philosophical Transactions of the Royal Society of London* **1834**, *124*, 77–122.

(113) Johnson, B. A., *Interrogating Diffusional Mass and Charge Transport in Catalytic Metal-Organic Frameworks*, 2020.

(114) Nicholson, R. S.; Shain, I. Theory of Stationary Electrode Polarography: Single Scan and Cyclic Methods Applied to Reversible, Irreversible, and Kinetic Systems. *Analytical Chemistry* **1964**, *36*, 706–723, DOI: 10.1021/ac60210a007.

(115) Andrieux, C. P.; Savéant, J.-M. Heterogeneous Chemically Modified Electrodes, Polymer Electrodes Vs. Homogeneous Catalysis of Electrochemical Reactions. *J. Electroanal. Chem* **1978**, *93*, 163.

(116) Costentin, C.; Savéant, J.-M. Multielectron, Multistep Molecular Catalysis of Electrochemical Reactions: Benchmarking of Homogeneous Catalysts. *ChemElectroChem* **2014**, *1*, 1226–1236, DOI: 10.1002/celc.201300263.

(117) Costentin, C.; Drouet, S.; Robert, M.; Savéant, J. M. Turnover numbers, turnover frequencies, and overpotential in molecular catalysis of electrochemical reactions. Cyclic voltammetry and preparative-scale electrolysis. *J. Am. Chem. Soc.* **2012**, *134*, 11235–11242, DOI: 10.1021/ja303560c.

(118) Savéant, J.-M.; Su, K. B. Homogenous Redox Catalysis of Electrochemical Reaction Part VI. Zone Diagram Representation of the Kinetic Regimes. *J. Electroanal. Chem* **1984**, *171*, 341–349.

(119) Savéant, J.-M. Molecular Catalysis of Electrochemical Reactions. Mechanistic Aspects. *Chem. Rev.* **2008**, *108*, 2348–2378, DOI: 10.1021/cr068079z.

(120) Costentin, C.; Savéant, J.-M. Homogeneous Catalysis of Electrochemical Reactions: The Steady-State and Nonsteady-State Statuses of Intermediates. *J. Am. Chem. Soc.* **2018**, *8*, 5286â5297, DOI: 10.1021/acscatal.8b01195.

(121) Costentin, C.; Nocera, D. G.; Brodsky, C. N. Multielectron, multisubstrate molecular catalysis of electrochemical reactions: Formal kinetic analysis in the total catalysis regime. *Proceedings of the National Academy of Sciences of the United States of America* **2017**, *114*, 11303–11308, DOI: 10.1073/pnas.1711129114.

(122) Lee, K. J.; McCarthy, B. D.; Dempsey, J. L. On decomposition, degradation, and voltammetric deviation: The electrochemist's field guide to identifying precatalyst transformation. *Chem. Soc. Rev.* **2019**, *48*, 2927–2945, DOI: 10.1039/c8cs00851e.

(123) Sequoia, E.; Andrieux, C. P.; Hapiot, P.; Savánt, J.-M. Repetitive Cyclic Voltammetry of Irreversible Systems. *J. Electroanal. Chem* **1993**, *349*, 299–309.

(124) C., A.; M., G.; J.M., S. Homogeneous vs. Heterogeneous Electron Transfer in Electrochemical Reactions: Application to the Electrohydrogenation of Anthracene and Related Reactions. *J. Electroanal. Chem.* **1983**, *147*, 1–38.

(125) Dainty, C.; Bruce, D. W.; Cole-hamilton, D. J.; Camilleri, P. The Photochemical Reduction of 2,1,3-Benzothiadiazole-4,7-dicarbonitrile by Ethylenediaminetetraacetic acid in the Presence of Micelles. *J. Chem. Soc., Chem. Commun.* **1984**, 1324–1325.

(126) Camilleri, P.; Dearing, A.; Cole-hamilton, D. J.; Neill, P. O. One-electron Reduction of 2,1,3-Benzothiadiazole-4,7-dicarbonitrile in Aqueous Solutions. *J. Chem. Soc. Perkin Trans.* **1986**, *104*, 569–572.

(127) Robinson, J. N.; Cole-hamilton, D. J.; Dainty, C.; Maxwell, V.; Camilleri, P. The Photochemical Reduction of 2,1,3-Benzothiadiazole-4,7- dicarbonitrile in the Presence of Cationic Micelles, and Onward Electron-transfer Reactions. *J. Chem. Soc. Faraday Trans.* **1989**, *85*, 3385–3394.

(128) Robinson, J. N.; Cole-hamilton, D. J.; Whittlesey, M. K.; Camilleri, P. Photochemical Electron Transfer Across Surfactant Bilayers Mediated by 2,1,3-Benzothiadiazole-4,7-dicarbonitrile. *J. Chem. Soc. Faraday Trans.* **1990**, *86*, 2897–2903.

(129) Kütt, A.; Leito, I.; Kaljurand, I.; Sooväli, L.; Vlasov, V. M.; Yagupolskii, L. M.; Koppel, I. A. A Comprehensive Self-Consistent Spectrophotometric Acidity Scale of Neutral Brnsted Acids in Acetonitrile. *J. Org. Chem.* **2006**, *71*, 2829–2838, DOI: 10.1021/jo060031y.

(130) Eckert, F.; Leito, I.; Kaljurand, I.; Kütt, A.; Klamt, A.; Diedenhofen, M. Prediction of Acidity in Acetonitrile Solution with COSMO-RS. *J. Comput. Chem* **2009**, *30*, 799–810, DOI: 10.1002/jcc.21103.

(131) Bryce, M. R. Use of Piperidine-1-sulphenyl Chloride as a Sulphur-transfer Reagent in Reactions with Diamines: The Preparation of Sulphur-Nitrogen Heterocycles. *J. Chem. Soc. Perkin Trans.* **1984**, *3*, 53–87.

(132) Soloway, S.; Lipschitz, A. Basicity of Some Nitrilated Amines. *J. Org. Chem.* **1958**, 613–615.

(133) Liu, A.; Tai, C. W.; Holá, K.; Tian, H. Hollow polymer dots: Nature-mimicking architecture for efficient photocatalytic hydrogen evolution reaction. *J. Mater. Chem.* **2019**, *7*, 4797–4803, DOI: 10.1039/c8ta12146j.

(134) Pavliuk, M. V.; Lorenzi, M.; Morado, D. R.; Gedda, L.; Wrede, S.; Mejias, S. H.; Liu, A.; Senger, M.; Glover, S.; Edwards, K.; Berggren, G.; Tian, H. Polymer Dots as Photoactive Membrane Vesicles for [FeFe]-Hydrogenase Self-Assembly and Solar-Driven Hydrogen Evolution. *J. Am. Chem. Soc.* **2022**, *144*, 13600–13611, DOI: 10.1021/jacs.2c03882.

(135) Wang, S.; Cai, B.; Tian, H. Efficient Generation of Hydrogen Peroxide and Formate by an Organic Polymer Dots Photocatalyst in Alkaline Conditions. *Angew. Chem. Int. Ed.* **2022**, *61*, e202202733, DOI: 10.1002/anie.202202733.

(136) Mustafa, A.; Shuai, Y.; Lougou, B. G.; Wang, Z.; Razzaq, S.; Zhao, J.; Shan, J. Progress and perspective of electrochemical CO2 reduction on Pd-based nanomaterials. *Chem. Eng. Sci.* **2021**, *245*, 116869, DOI: 10.1016/J.CES.2021.116869.

(137) Duan, L.; Uddin, A. Progress in Stability of Organic Solar Cells. *Adv. Sci.* **2020**, *7*, 19032595, DOI: 10.1002/advs.201903259.

(138) Seshadri, G.; Lin, C.; Bocarsly, A. B. A new homogeneous electrocatalyst for the reduction of carbon dioxide to methanol at low overpotential. *J. Electroanal. Chem* **1994**, *372*, 145–150, DOI: 10.1016/0022-0728(94)03300-5.

(139) Costentin, C.; Saveánt, J.-M.; Tard, C. Catalysis of CO 2 Electrochemical Reduction by Protonated Pyridine and Similar Molecules. Useful Lessons from a Methodological Misadventure. *ACS Energy Lett.* **2018**, *3*, 695–703, DOI: 10.1021/acsenergylett.8b00008.

(140) Lim, C.-H.; Holder, A. M.; Musgrave, C. B. Mechanism of Homogeneous Reduction of CO2 by Pyridine: Proton Relay in Aqueous Solvent and Aromatic Stabilization. *J. Am. Chem. Soc.* **2012**, *135*, 142–154, DOI: 10.1021/ja3064809.

(141) Lucio, A. J.; Shaw, S. K. Pyridine and Pyridinium Electrochemistry on Polycrystalline Gold Electrodes and Implications for CO2 Reduction. *J. Phys. Chem. C.* **2015**, *119*, 12523–12530, DOI: 10.1021/acs.jpcc.5b03355.

(142) Dunwell, M.; Yan, Y.; Xu, B. In Situ Infrared Spectroscopic Investigations of Pyridine-Mediated CO2 Reduction on Pt Electrocatalysts. *ACS Catalysis* **2017**, *7*, 5410–5419, DOI: 10.1021/acscatal.7b01392.

(143) Khan, J.; Sun, Y.; Han, L.; Khan, J.; Han, L.; Sun, Y. A Comprehensive Review on Graphitic Carbon Nitride for Carbon Dioxide Photoreduction. *Small Methods* **2022**, *6*, 2201013, DOI: 10.1002/smtd.202201013.

(144) Dai, C.; Zhong, L.; Gong, X.; Zeng, L.; Xue, C.; Li, S.; Liu, B. Triphenylamine based conjugated microporous polymers for selective photoreduction of CO 2 to CO under visible light. *Green Chemistry* **2019**, *21*, 48–89, DOI: 10.1039/c9gc03131f.

(145) Wang, S.-H.; Chen, P.-Z.; Chen, Y.-Y.; Khurshid, F.; Cai, C.-W.; Lai, Y.-Y.; Chung, P.-W.; Jeng, R.-J.; Rwei, S.-P.; Wang, L. Naphthalene Diimide-Based Donor-Acceptor-Donor Small Molecules as Metal-Free Organocatalysts for Photocatalytic CO2 Reaction. *ACS Appl Mater Interfaces* **2022**, *14*, 43109–43115, DOI: 10.1021/acsami.2c08531.

(146) Lei, K.; Wang, D.; Ye, L.; Kou, M.; Deng, Y.; Ma, Z.; Wang, L.; Kong, Y. A Metal-Free Donor-Acceptor Covalent Organic Framework Photocatalyst for Visible-Light-Driven Reduction of CO2 with H2O. *ChemSusChem* **2020**, *13*, 1725–1729, DOI: 10.1002/cssc.201903545.

(147) Wang, S.; Hai, X.; Ding, X.; Jin, S.; Xiang, Y.; Wang, P.; Jiang, B.; Ichihara, F.; Oshikiri, M.; Meng, X.; Li, Y.; Matsuda, W.; Ma, J.; Seki, S.; Wang, X.; Huang, H.; Wada, Y.; Chen, H.; Ye, J. Intermolecular cascaded π-conjugation channels for electron delivery powering CO2 photoreduction. *Nat. Commun.* **2020**, *11*, 1149, DOI: 10.1038/s41467-020-14851-7.

(148) Song, X.; Meng, Y.; Zare, R. N. Spraying Water Microdroplets Containing 1,2,3-Triazole Converts Carbon Dioxide into Formic Acid. *J. Am. Chem. Soc* **2022**, *144*, 16744–16748, DOI: 10.1021/jacs.2c07779.

(149) Boot-Handford, M. E.; Abanades, J. C.; Anthony, E. J.; Blunt, M. J.; Brandani, S.; Dowell, N. M.; Fernández, J. R.; Fernández, F.; Ferrari, M.-C.; Gross, R.; Hallett, J. P.; Haszeldine, R. S.; Heptonstall, P.; Lyngfelt, A.; Makuch, Z.; Mangano, E.; Porter, R. T. J.; Pourkashanian, M.; Rochelle, G. T.; Shah, N.; Yao, J. G.; Fennell, P. S. Carbon capture and storage update. *Energy Environ. Sci.* **2014**, *7*, 130–189, DOI: 10.1039/c3ee42350f.

(150) Barlow, J. M.; Clarke, L. E.; Zhang, Z.; Bí, D.; Ripley, K. M.; Zito, A.; Brushett, F. R.; Alexandrova, A. N.; Yang, J. Y. Molecular design of redox carriers for electrochemical CO 2 capture and concentration. *Chem. Soc. Rev* **2022**, *51*, 8415, DOI: 10.1039/d2cs00367h.

(151) Iijima, G.; Naruse, J.; Shingai, H.; Usami, K.; Kajino, T.; Yoto, H.; Morimoto, Y.; Nakajima, R.; Inomata, T.; Masuda, H. Mechanism of CO2 Capture and Release on Redox-Active Organic Electrodes. *Energy Fuels* **2023**, *37*, 2164–2177, DOI: 10.1021/acs.energyfuels.2c03391.

(152) Williams, D. B. G.; Lawton, M. Drying of Organic Solvents: Quantitative Evaluation of the Efficiency of Several Desiccants. *J. Org. Chem.* **2010**, *75*, 8351–8354, DOI: 10.1021/jo101589h.

(153) Johnson, B. A.; Agarwala, H.; Hite, T. W.; Mijangos, E.; Maji, S.; Ott, S. Judicious Ligand Design in Ruthenium Polypyridyl CO 2 Reduction Catalysts to Enhance Reactivity by Steric and Electronic Effects. *Chem. Eur.J* **2016**, *22*, 14870–14880, DOI: 10.1002/chem.201601612.

(154) Angamuthu, R.; Byers, P.; Lutz, M.; Spek, A. L.; Bouwman, E. Electrocatalytic CO2 conversion to oxalate by a copper complex. *Science* **2010**, *327*, 313–315, DOI: 10.1126/science.1177981.

Acta Universitatis Upsaliensis

Digital Comprehensive Summaries of Uppsala Dissertations from the Faculty of Science and Technology 2297

Editor: The Dean of the Faculty of Science and Technology

A doctoral dissertation from the Faculty of Science and Technology, Uppsala University, is usually a summary of a number of papers. A few copies of the complete dissertation are kept at major Swedish research libraries, while the summary alone is distributed internationally through the series Digital Comprehensive Summaries of Uppsala Dissertations from the Faculty of Science and Technology. (Prior to January, 2005, the series was published under the title "Comprehensive Summaries of Uppsala Dissertations from the Faculty of Science and Technology".)

Distribution: publications.uu.se
urn:nbn:se:uu:diva-509537

ACTA UNIVERSITATIS
UPSALIENSIS
2023